5-2013

# Investigation of the Mechanism Underlying Arsenic Disruption of Mast Cell Degranulation

Alejandro Velez
*University of Maine - Main*

# INVESTIGATION OF THE MECHANISM UNDERLYING ARSENIC DISRUPTION OF MAST CELL DEGRANULATION

by

Alejandro Velez

A Thesis Submitted in Partial Fulfillment
of the Requirements for a Degree with Honors
(Biochemistry)

The Honors College

University of Maine

May 2013

Advisory Committee:

Julie A. Gosse, PhD, Assistant Professor, Biochemistry, Advisor
James E. Gallagher, PhD, Associate Professor Emeritus, Sociology, Honors Faculty
Carol Kim, PhD, Professor, Molecular & Biomedical Sciences, Director, Graduate School of Biomedical Sciences
Charles E. Moody, PhD, Associate Professor, Molecular and Biomedical Sciences
Robert Gundersen, PhD, Chair & Associate Professor, Molecular & Biomedical Sciences

**Abstract**

Exposure to arsenic (As) is a global health concern, according to the World Health Organization and Agency for Toxic Substances and Disease Registry. Prolonged exposure to this naturally occurring chemical has been linked to hyperkeratosis, type II diabetes, developmental abnormalities, and cancer. Some of the adverse health effects of As may be linked to its ability to alter cellular signal transduction. Recently, published work from the Gosse laboratory has shown that inorganic arsenite inhibits the signaling cascade leading to mast cell degranulation, a vital immune function, through an as-yet unknown mechanism.

Further work in the Gosse lab has suggested that arsenic's effect occurs early in the degranulation signaling pathway, between receptor aggregation and calcium influx. Alternate FcεRI cross-linking methods produced similar As inhibition patterns, suggesting an As effect downstream of receptor aggregation. Calcium ionophore and compound 48/80-mediated degranulation responses were not inhibited by As-- evidence that arsenic's effect occurs upstream of calcium influx as well. This thesis will concentrate on testing the hypothesis that As disrupts antigen-stimulated tyrosine phosphorylation of Syk kinase, a signaling molecule functioning between receptor aggregation and calcium influx in mast cells. Using a piceatannol-arsenic combination assay it was found that Syk and piceatannol, a competitive inhibitor of Syk, cause an additive inhibitory effect on degranulation. Preliminary Phospho-Syk ELISA data provides evidence that arsenic may be interfering with the phosphorylation of Syk, a vital process during the development of hypersensitivity. Taken together, these data provide insight into possible mechanisms of toxicity of arsenic as well as a possible drug target in the treatment and prevention of asthma and allergy.

**Acknowledgments**

I would like to thank all of my co-workers and friends that made this thesis possible. My lab mates Andrew Abovian, Hina Hashmi, Lisa Weatherly, Kayla Blais, and Zachary Tranchemontagne, I am grateful for your support and your commitment to our lab. I would like to specifically thank Juyoung Shim for her contribution to this thesis with the Syk gene alignment analysis. I would also like to include the most sincere thanks to Dr. Julie A. Gosse and Rachel Kennedy for you devotion to always teach me something new and the valuable emotional, professional and scientific guidance that you provided through this thesis process. Finally, I would like to thank my entire brotherhood of Iota Nu Kappa for your unconditional emotional support and inspirational perspectives. Of special mention I would like to thank Richard Luc for his advice and insight through the research and the writing of this thesis. Without you all, this thesis, and the lessons I have learned through writing it, would have not been possible

THANK YOU!

**Table of Contents**

**List of Figures**

# 1. Introduction

## 1.1. Arsenic

Arsenic (As) is a metalloid commonly found in the Earth's crust at an average concentration of 2mg/ kg and as high as 100mg/kg as part of copper or lead ores, and within minerals in the soil [1]. Elemental arsenic, insoluble in water, is most commonly found in the environment combined with oxygen, sulfur, and chlorine, and is known as inorganic arsenic in this form. The most common arsenic-containing mineral in the soil is arsenopyritein (FeAsS), but arsenic is known to be associated with more than 200 different other minerals, especially those containing sulfide [1, 2, 3]. In the environment, inorganic arsenic can assume two valence states described as arsenite (As(III)) and arsenate (As (V)) [4]. Under reducing conditions the trivalent form is most prevalent, while in highly oxygenated environments (oxidizing conditions), the pentavalent form predominates [1]. Its trivalent form, arsenite, has been shown to be the more toxic of the two even in its monomethylated state [5]. The methods for possible toxicity will be discussed in later sections.

Sources of arsenic are varied and plentiful. Humans can come in contact with arsenic through the consumption of contaminated water and food, inhalation of industrial emissions from copper or lead smelting, as well as routine occupational exposure. For the general population, the most relevant exposure to arsenic is through the consumption of contaminated drinking water from wells located near mineral deposits [1, 6]. The levels of arsenic in drinking water vary by region but are estimated to range between 1 and 1000

ppb (µg/L). However, in areas such as West Bengal, India, Bangladesh, North Mexico, Chile and Argentina millions of people are affected by levels of arsenic in their drinking water ranging from 50 to 3000 ppb (µg/L)[1, 6]. Areas near sulfide mineralization and geochemical sites near Taiwan reported groundwater level of arsenic as high as 1 ppm (mg/L) [7].

Contaminated drinking water is the major source of arsenic exposure in humans, but consumption of arsenic-bearing foods like shellfish, cereals, and vegetables can also be a substantial source. A study of inorganic arsenic in the typical Hong Kong diet found levels of arsenic as high as 74 µg/kg (this is elemental arsenic per wet body weight; comparable to ppb) in water spinach, and 58 µg/kg (58 ppb) in oysters [9]. The highest arsenic-exposure contributing products were cereals with 53.5% contribution to the diet of the average Hong Kong citizen, with brown (unpolished) rice having the highest concentration of arsenic at 43 µg/kg (43 ppb). The study concluded that the high levels of arsenic in these foods are likely due to their aquatic growing conditions [9]. These Hong Kong study is one only of many similar studies attempting to elucidate the human dietary exposure to arsenic. Closer to home, the Consumer Reports magazine did a study of their own. Similar to the Hong Kong study, it was found that cereals were the largest contributor of arsenic with uncooked rice topping the charts at levels as high 900 ppb (900 µg/mL) [10]. Levels of arsenic in food this high are cause for concern given the major health problems that are linked to chronic exposure of arsenic.

### 1.2. Arsenic & Human Health

Due to its high prevalence in the environment, there has been a lot of attention on how exposure to arsenic affects the human body. Acute arsenic exposure (acute poisoning) can occur when the digestion of large amounts (>5mg) of arsenic containing products, such as insecticides, occurs. One-time doses of about 5mg of arsenic are described as causing minor complications such as vomiting and diarrhea; however, doses ranging from 100mg to 300mg can cause skin rashes, cardiomyopathy, seizures, renal failure, pulmonary edema and eventually death [11]. Acute poisoning of arsenic is rare and often accidental; however, chronic consumption of small doses (for example, 50 µg/L (or 50 ppb) in drinking water) of arsenic is just as dangerous and a more prevalent issue worldwide. Long term exposure to low levels of arsenic has been linked to health issues ranging from hyperpigmentation and keratosis to an increased risk of cardiovascular disease, respiratory disease, diabetes mellitus, and cognitive impairment [1, 11]. Chronic exposure to arsenic, however, has been most clearly linked with cancer development in nearly all organ systems of the body [1, 11, 12]. The U.S Environmental Protection Agency released a statement claiming that a lifetime exposure to arsenic as low as 1 ppb has been linked to having a significantly higher risk of developing skin cancer [6]. It is clear, then, that due to the high prevalence of arsenic in the environment and the large number of health concerns linked to arsenic exposure, the mechanism of toxicity warrants heavy scientific concern.

### 1.3. Arsenic & Cell Signaling

Some of the adverse health effects of As may be linked to its ability to alter cellular signal transduction [13, 14]. Arsenic has been linked with the formation of harmful reactive oxygen species (ROS) and the disruption of tyrosine phosphorylation in

many cell lines and model organisms [4, 13, 14, 15, 16, 17]. Arsenic-induced ROS formation has been shown to cause DNA damage and protein alteration. In a study using $A_L$ human-hamster hybrid cells a significant increase in ROS production was observed within the first 5 min of exposure [20]. Furthermore, a decrease in nonprotein sulfhydryls caused a 5-fold increase in intragenic and multilocus deletion mutations in the DNA of these cells providing strong evidence for possible mechanistic routes of cancer development induced by arsenic [20]. Additionally, it has been well documented that As can have adverse effects on phosphorylation pathways [4, 13, 16, 17, 18]. For example, As has been linked with a significant decrease in cytokine production (IL-2) of splenic mononuclear cells in male mice [15]. This disruption of T-cell activation was concluded to be linked with an increase in the levels of phosphorylation of the early protein tyrosine phosphorylation cascade proteins that included Lck and Fyn kinases [15].Whether this effect is through the substitution of phosphate groups by the isostructural compound arsenate [13, 16, 18], the ability of arsenite to interact with sulfhydryl groups [13], or arsenite's ability to form reactive oxygen species that inactivate kinases or phosphatases [13,16], or some other mechanism, it is evident that the next logical step would be to focus our research on the early phosphorylation events of cell signaling.

### 1.4. Mast Cells & RBL-2H3 Cell Line

The mast cell, as a key player in parasite defense and the allergy response, is an important cell line to keep in mind through the evaluation of arsenic exposure and its effects. Mast cells, as leukocytes, play a major role in defense against pathogens and are derived from haematopoietic progenitor cells [8, 19, 21]. Prior to maturation within the mucosal and connective tissues, mast cells circulate through the vascular system as

progenitors following a model of development similar to that of a macrophage [8, 19]. A specific progenitor has only been successfully identified in fetal blood and they are described as expressing the cluster of differentiation (CD) molecules, CD34, CD117 (c-kit), and CD13 in humans and Thy-$1^{lo}$c-$kit^{hi}$ cell in mouse [8, 22]. However, the cell progenitors identified in this study lacked the expression of the FcεRI receptor that is often associated with parasite defense, and FcεRI expression was only induced via experimental methods *in vivo* and *in vitro*, thus an appropriate mast cell progenitor still has yet to be identified [8].

Mast cells contribute to the defense against parasites via the degranulation process, in which compounds meant to fight off parasitic infection are released from the cells' intracellular granules. Activation of this degranulation pathway is triggered by antigen, or allergen, from a foreign organism, which crosslinks IgE-bound FcεRI receptors, thus triggering an internal signaling pathway eventually leading to the release of pro-inflammatory meditators through degranulation [23, 24, 25, 26, 27]. Antigen stimulation sets in motion a cascade of tyrosine phosphorylation events that notably include the kinases Lyn and Syk [23, 24, 25, 28, 29, 30], among others. The phosphorylation of the receptor and the kinases leads to calcium influx and the mobilization and fusion of mediator-filled granules with the plasma membrane [23, 24, 25, 28, 29]. Within these aformentioned pre-formed granules we find the mediators histamine, a well described player in the allergic response, tryptase and chymases (proteases), tumor necrosis factor-alpha and many other cytokines that are found to be vital in the non-specific branch of the immune system [19, 25, 23]. More detail will be included in the "degranulation pathway" section.

The degranulation pathway has been extensively studied through the use of Rat Basophilic Leukemia (RBL) cells as model for basophils, due to their reliable release of histamine through the stimulation of FcεRI receptors [31] and their functional similarity to primary human basophils and rodent mast cells [32, 33]. In the literature, the RBL-2H3 cell line has been described as sharing functional and phenotypic similarities with basophils and mast cells [34]. The 2H3 cell line has been shown to respond in a similar fashion to the calcium ionophore A23187, as do basophils and mast cells [34]. Much like basophils and mast cells, RBL-2H3 release β-hexosaminidase, an exoglycosidase, from the granules in parallel with histamine and the other mediators, which lends itself as way to quantify degranulation [34, 35]. The presence of Toll Like Receptor 4 (TLR4) on the cell surface of both RBL-2H3 and basophils attributes to their similarity; however, unlike basophils, RBL-2H3 are unable to respond to bacterial lipopolysaccharide membrane component that has been shown to interact heavily with TLR4 [34]. Furthermore, RBL-2H3 has been shown to switch phenotypes depending on the current microenvironment in which they reside [34] This has been shown by Swieter *et al* by culturing RBL-2H3 cells with 3T3 fibroblast that lead to a switch from compound 48/80 insensitive RBLs to sensitive ones [37].Although RBLs are well accepted as models of basophils and mast cells, they differ in some phenotypical aspects. For example, RBL cell lines have been shown to express a different density of FcεRI receptors at the plasma membrane [36]. Given this information we have chosen to use the RBL-2H3 cell line for our investigation of arsenic's effects on mast cell degranulation with the reservation that as Passante *et al* puts it, "RBL-2H3 cells resemble MMC in some respects, and display their basophilic lineage in others, their true nature lies somewhere in between [34]."

### 1.5. Mast Cell Degranulation

Activating the degranulation pathway requires the binding of an antigen, a molecule that elicits an immune response, to the corresponding IgE antibody. This antibody must first be produced by the workhouse of the immune system, the B cell. When an antigen enters the body it is challenged by an antigen presenting cells, most often a dendritic cell, which recognizes the antigen as foreign, integrates it, processes it and presents it via its Major Histcompatibility Complex molecule [38]. This dendritic cell migrates to the local lymph-node where it encounters a naïve CD4+ T-helper lymphocyte ($T_H$ cell) that promotes a cytokine exchange and the maturation, and differentiation, of the naïve $T_H$ cell to an antigen-specific $T_H2$ cell [39]. Once activated these antigen-specific $T_H2$ cell can interact with a cognate B-cell to stimulate the upregulation of CD80/CD86 and CD40 ligands on the $T_H2$ cell. Along with the cytokines secreted by both parties involved, these changes induce the B cell to proliferate into short lived plasma cells that immediately produce IgM antibodies. Shortly after, however, these activated B-cells undergo class switch recombination (stimulated by the CD40 ligation signals and the cytokines IL-4/IL-13) in which a complex process of rearrangement at the immunoglobulin heavy chain locus, and an excision and ligation of the DNA, gives rise to the antigen-specific IgE antibody [38]. Once the class switch recombination is complete, these antigen-specific B cell continue to proliferate into memory cells and the IgE producing plasma cells.

The short lived, often less than 3 days, IgE antibodies circulate the tissues to which they are sequestered and encounter the FcεRI receptor of an un-sensitized mast cell [40]. Although the FcεRI is constitutively expressed in mast cells [24, 41, 42], the high

affinity binding of IgE antibodies upregulates the cell-surface expression of the FcεRI expression and inhibits the internalization of unbound receptors on the surface [24]. The high affinity receptor for IgE, or FcεRI, is a membrane-bound tetrameric complex consisting of the IgE binding α chain, a membrane tetraspanning signal-amplifying β chain and the disulfide-linked homodimer γ chain that provides the signaling ability to the receptor [23, 24, 25, 41]. An important fact to note is that murine and human models differ in their β-chain requirement during receptor expression. Expression of FcεRI in humans can include the tetrameric form ($\alpha\beta\gamma_2$) or the trimeric form ($\alpha\gamma_2$) and does not require β chain expression for cell-surface expression like the rodent model does [43]. Rodent FcεRI is strictly found in its tetrameric form and the co-expression of the β-chain is vital for receptor expression [24, 43]. In both models, the constant (Fc) region of one free-floating IgE binds to the extracellular portion of a single α chain of a FcεRI receptor with an affinity of $1 \times 10^{10}$ $M^{-1}$ [43, 44].

Upon the 1:1 binding of IgE to FcεRI receptor, the mast cell is said to be sensitized [45]. A sensitized mast cell can now respond to a specific antigen by binding the multivalent antigen to multiple receptor-bound IgEs, causing crosslinking and aggregation of receptors, which initiates the signal transduction pathway leading to degranulation [23, 24, 45]. Aggregation of the receptors activates the protein tyrosine kinase (PTKs) Lyn, bound to the β chains of each receptor, which immediately goes on to phosphorylate the immunoreceptor tyrosine-based activation motifs (ITAMs) of the receptor neighboring it; this model is known as the transphosphorylation model [46, 47]. There is, however, some dispute as to whether this transphosphorylation model or a lipid raft based model is at work. The lipid raft model claims that, upon aggregation of the

receptors, the aggregated receptors and Lyn (which is tethered to the plasma membrane via palmitoyl and myristoyl anchors) both favor and are clustered together in cholesterol- and saturated fat-rich, detergent resistant microdomains (DRMs). In these small, specialized regions of the membrane, Lyn and the aggregated receptors are in close enough proximity to allow Lyn to carry out the phosphorylation of the β and γ chains of the receptors. In fact, Lyn is more enzymatically active inside DRMs than outside because of exclusion of certain phosphatases from lipid rafts [48].

Regardless of the model, Lyn has been shown to have a regulatory role during these early events. Xiao *et al* used BMMCs with a combination of IgE + anti-IgE, IgE+ low antigen, and IgE + high antigen treatments and found that the activity of Lyn as well as its association with FcεRI β subunit was suppressed upon low intensity stimulation, while high intensity stimulation caused enhanced Lyn activity and higher levels of phosphorylated FcεRI β subunit and Syk kinase [30].

The ITAMs phosphorylated by Lyn consist of an 18–amino acid motif (E/DxxYxxLxxxxxxx-YxxL) found on the β and γ chains of each FcεRI receptors; the ITAMs are crucial to the initiation of the degranulation pathway [43]. Although activation of Lyn is agreed to be the step following receptor aggregation and eventually degranulation, it is not the only one. In fact, Lyn-deficient bone-marrow-derived mast cells showed normal degranulation suggesting a parallel, compensational pathway [49]. It was later determined that this complementary pathway included the PTK Fyn, known for maintenance and amplification of calcium ($Ca^{+2}$) signaling [23, 24], however, in this study we will concentrate on the primary Lyn pathway.

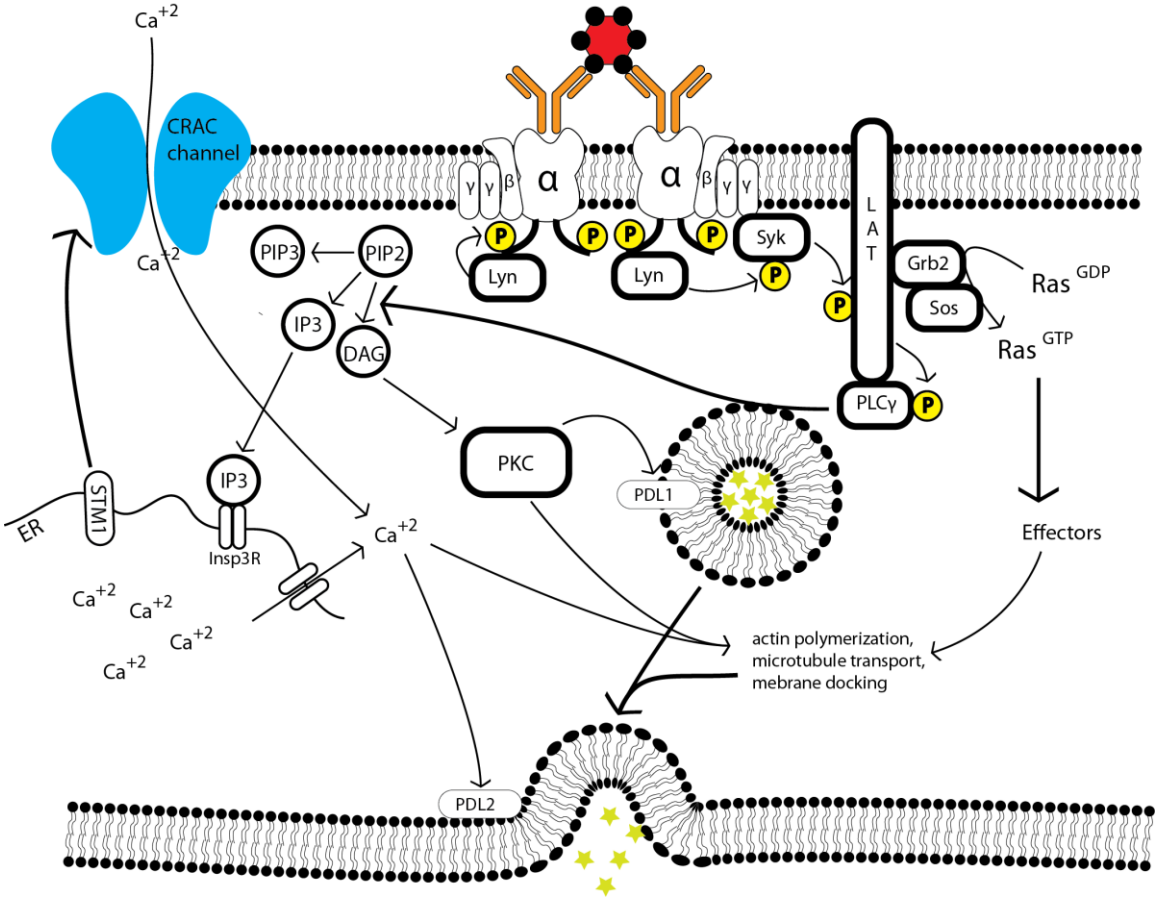


**Figure 1: Schematic of the Degranulation Model**

Picture was adapted from previous graphics made by Jonathan Pelletier and Rachel Kennedy. Created in Adobe Illustrator CS5.

The phosphorylation of the β and γ chains of the ITAMs by Lyn serve as docking sites for Src Homology 2 (SH2) domains of the PTK Syk. Syk binds to the phosphorylated γ chains and becomes activated, via a conformational change, after being phosphorylated by Lyn [31, 43]. For more information on Lyn and Syk please refer to their dedicated sections below. Lyn and Syk activation mark a divergence point on several signaling pathways that include the production of cytokines, eiscosanoids, growth factors and, as will be the topic of the remainder of this discussion, degranulation [24,

42]. Following the degranulation pathway, activated Syk phosphorylates LAT (linker for activation of T cells) at four distinct residues (Y171, Y191, Y226 and Y132) that allow it to act as a scaffold for phospholipase Cγ1 (PLCγ1) [25, 50]. Once bound, PLCγ1 is phosphorylated and activated by Syk, which is followed by the hydrolysis of phosphatidylinositol-4,5-bisphosphate (PIP2) to inositol-1,4,5-triphosphate (IP3) and diacylglycerol (DAG) [25, 44]. The lipid mediator IP3 induces the release of intracellular stores of $Ca^{+2}$ via the IP3 receptor (Insp3R) found on the endoplasmic reticulum membrane, while at the same time, DAG activates the serine/threonine protein kinase C (PKC) [24, 25, 51,52]. Once endoplasmatic $Ca^{+2}$ stores are emptied, the STIM1 protein, a $Ca^{+2}$ sensor found on the ER membrane, is relocated to the plasma membrane where it interacts with store-operated $Ca^{+2}$ (SOC) influx via $Ca^{+2}$- release-activated $Ca^{+2}$ (CRAC) channels [53, 54]. This STIM1 protein possesses an amino-terminal EF hand $Ca^{+2}$ binding domain that upon depletion of ER $Ca^{+2}$ leads to rapid translocation to the plasma membrane [55]. A study found that point mutations on the $Ca^{+2}$ binding domain of STIM1 resulted in failure to promote SOC influx of $Ca^{+2}$ in response to ER store depletion [54, 55]. Free $Ca^{+2}$ and activated PKC act synergistically to assemble and aid the machinery necessary for granule fusion with the membrane. PKC has been found to phosphorylate both the light and heavy myosin chains, which contribute to the necessary rearrangement of the cortical barrier in order for vesicle fusion to occur [56, 57]. Furthermore, it has also been shown that $Ca^{+2}$/Calmudulin-dependent protein kinase II phosphorylates also phosphorylates the heavy myosin chain during this exocytosis process [57, 58].

Exocytosis of the mediator-filled granules requires a complex machinery to fuse the vesicle (granule) with the cell membrane. In mast cells this process is facilitated by soluble NSF (N-ethyl-maleimidesensitive factor) attachment protein receptors (SNAREs) that are found on the vesicle and the cell membrane [41, 59]. These SNAREs interact with each other to form a complex that brings both membranes to a distance that will allow for fusion to occur [59]. The membrane of the granule is equipped with a vesicle-associated membrane protein (VAMP), a SNARE that has been found in many isoforms including VAMP 2, 3,7 or 8 [41, 60, 61]. It is not known, however, which isoform participates specifically during IgE mediated degranulation. The cell membrane contains SNAP 23, a ubiquitous SNARE, and syntaxin 4, another SNARE often associated with IgE mediated degranulation [41,61]. Along with these SNAREs we also see many accessory proteins such as NSF ATPase, for disassembly, and Rab GTPases involved in regulation of the complex [41, 62]. In the presence of free calcium, a calcium sensor (calmodulin or a synaptotagmin) binds directly to VAMP-2 and liberates it from its lipid-bound state. Simultaneously, PKC phosphorylates SNAP 23 and syntaxin 4, which causes a rearrangement of cytoskeletal components that interact with the freed VAMP-2 to form the granule fusion complex [41, 59]. Once assembled, the presence of calcium allows for the vesicle and the membrane to come to a distance of 2–3 Å, which energetically favors the fusion of the membranes and the exocytosis of the mediators [59]. The PKC and DAG complex are also known to regulate phospholipase D (PLD), which plays a vital role in granule fusion with the cell membrane. PLD presents itself in two isoforms, PLD1 and PLD2 that are found on the granule and the plasma membrane, respectively [63].

### 1.6. Lyn Kinase

Lyn is a known member of the Src family of intracellular membrane-associated tyrosine kinases that are composed of a unique N-terminal myristoylation and palmitoylation site, two homologous protein interaction domains (SH2 and SH3), and a C-terminal kinase domain [64]. Studies have shown two important regulating residues located on the kinase domain: Tyrosine (Y) residue 397, when phosphorylated, activates kinase activity [65] while Y508, when phosphorylated, inactives Lyn [66]. Lyn normally favors its inactive or closed conformation. This closed interaction is mediated through the negative regulatory tyrosine (Y508) at the COOH-terminus that interacts with Lyn's own SH2 domain causing the protein to collapse into itself. A C-terminal Src kinase (Csk) is responsible for phosphorylating Y508 and keeping Lyn in its inactive conformation [66]. Upon FcεRI stimulation, the balance between Csk and CD45 shifts, and the phosphatase CD45 acts to reverse the phosphorylation of Y508 which allows Lyn's SH2 domain to bind to the receptor and cause a conformational change that exposes its activation loop containing Y397. Phosphorylation of this residue activates the kinase activity of Lyn and allows Lyn to phosphorylate the receptor, and eventually Syk [67]. The role of Lyn is often described as a positive regulator of degranulation, but recent studies have shown that Lyn plays an important negative regulation role as well. Lyn has been shown to regulate the levels of PIP3 by inhibiting SH2 domain-containing inositol phosphatase-1 (SHIP-1) to control the extent of degranulation [67, 68]. Lyn as also been show to inhibit the Fyn-dependent pathway by phosphorylating Cbp (C-terminal Src kinase (Csk)-binding protein), allowing Csk to bind and to inhibit Fyn kinase via a mechanism similar to that needed to maintain Lyn's closed conformation [67, 69]. As a kinase vital to the degranulation pathway, Lyn is a possible target for arsenic's inhibitory effects.

### 1.7. Syk Kinase

Like Lyn, Syk is another key PTK involved in the degranulation pathway that could be a possible target for arsenic inhibition. Syk is part of the SYK family of tyrosine kinases that contain a C-terminal kinase domain and a tandem N-terminal SH2 domains (Figure 2 A) [50, 70, 71]. ZAP-70 and Syk, both members of the SYK family of tyrosine kinases, possess a linker region that separates these domains termed interdomain1, however, Syk has an additional 23 amino acid linker region called interdomain B that differentiates it from ZAP-70 [70, 71]. Due to these structural differences ZAP-70 and Syk have important functional differences. Syk, unlike ZAP-70, is capable of phosphorylating ITAMs without the help of Fyn or Lyn (Src kinases) [72]. Furthermore, Syk has the ability to transphosphorylate neighboring Syk molecules while ZAP-70 requires activation via the phosphorylation of its Y493 residue by Src kinase to do so [73, 74]; transphosphorylation is a key aspect of signal amplification. Syk, as stated above in the "degranulation" section, binds to phosphorylated γ chain ITAMs and becomes activated via a conformational change in which the linker region folds the molecule so that the SH2 domains are adjacent to the kinase domain. This conformation stabilizes the structure of Syk and exposes residues Y519 and Y520 to Lyn phosphorylation or, if Lyn is absent, to autophosphorylation [50, 71]. Phosphorylation of key resides Y317, Y342 and Y346 in the linker region allows for docking, and eventually the activation, of downstream targets of Syk such as LAT, Vav and SLP-46 [29]. Syk is an essential kinase in the activation of PLCγ and $Ca^{+2}$ release: Zhang *et al* found that in Syk-deficient TBIA2 (a cell line derived from RBL-2H3 cells) cells there was no appreciable tyrosine phosphorylation of PLCγ1/2 and no detectable rise in intracellular $Ca^{+2}$ upon receptor

aggregation. Furthermore, this study showed that transfection of Syk into these Syk-deficient cells rescued the activation of PLCγ and $Ca^{+2}$ influx [75]. Another study by Grodzki *et al* found that degranulation and cytokine production requires Syk as Syk deficient RBLs were not able to degranulate or activate NFAT (nuclear factor of activated T cells; transcription factors observed during $Ca^{+2}$ fluctuations in degranulation) [76].

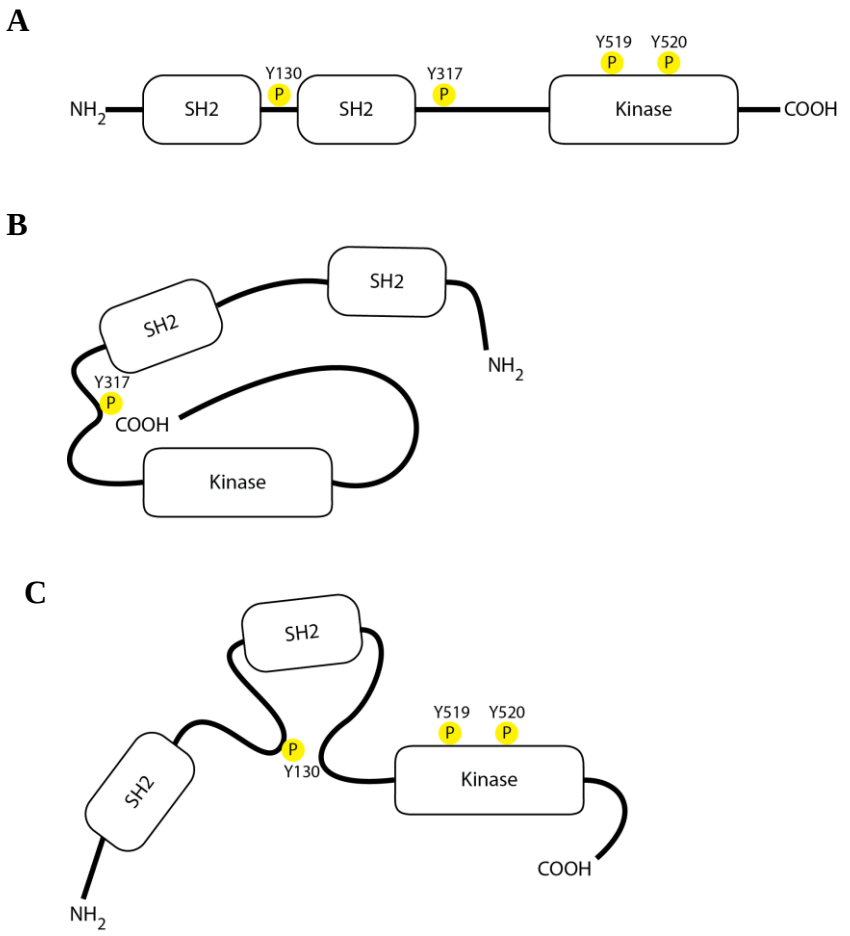


**Figure 2: Schematic Diagram of Syk and its States of Activity**

(A) Linear structure of Syk with phosphorylated tyrosine residues mentioned in the text. (B) Autoinhibited structure of Syk with phosphorylated Y317 negatively regulating the activity of Syk. (C) Activated structure of Syk with phosphorylated Y130, Y519, and Y520, which positively regulate Syk. Diagrams are adopted from Figure 1 of (De Castro, 2011). Created using Adobe Illustrator CS5.

As a vital player in degranulation, Syk is tightly regulated. Syk exists primarily in its autoinhibitory state that is stabilized by a hydrophobic area composed of Pro(P)-396, Y397 and Y474 in the kinase domain and Y319 in the linker region [77]. Upon coming in contact with, and binding to, the Lyn-phosphorylated γ chain of the FcεRI receptor, the hydrophobic interactions are disrupted, and Syk becomes activated. During the interaction between the SH2 domains of Syk and the phosphorylated ITAMs of the receptor, the residue Y130 on the linker region between the tandem SH2 domains of Syk plays a vital role in regulating the successful association between the two. Phosphorylation of Y130 dissociates Syk from the receptor by increasing the physical distance between the SH2 domains and preventing appropriate binding to the phosphorylated residues of the receptor [77]. Phosphorylation of Y317, found in interdomain 2, has been shown to negatively regulate Syk activity as well. In a study reviewed in de Castro *et al*, the expression of Syk-Y317F increased the activation of PLCγ1/2 and enhanced the degranulation of the cells; replacing Y317 with a Phe showed similar data as well (Figure 2 B) [77]. The positive regulation of Syk is varied and extensive; however, the phosphorylation of residues, via autophosphorylation or another kinase, Y519 and Y520 is necessary for signal transduction (Figure 2 C) [77]. Additionally, Zhang *et al* found that the replacement of either, or both, residues with Phe did not inhibit kinase activity, but it did hinder signal transduction as the levels of total tyrosine phosphorylation were considerably lower than the wild type controls [77, 78]. Much like Lyn, Syk is an essential PTK in the degranulation pathway that is strictly

regulated and presents an attractive location for arsenic induced inhibition of mast cell degranulation.

### 1.8. Current Work

The Gosse Lab has reported on the suppressive, dose-dependent effect of As on mast cell degranulation at doses that are environmentally relevant [79]. They showed that antigen activation of the cells was necessary for As to have any effect. Second, alternate FcεRI cross-linking methods (other than multivalent antigen) produced similar degranulation and As inhibition patterns [79]; this result provides evidence that As is not directly disrupting the interaction between the receptor-bound IgE and the crosslinker (either multivalent antigen or anti-IgE antibody). In order to assess whether arsenic's effect occurs downstream or upstream of calcium influx, Hutchinson and others used calcium ionophore to achieve degranulation while bypassing the FcεRI receptor and the early tyrosine phosphorylation cascade. Their results showed that As, in fact, did not affect ionophore induced degranulation, and, thus, As must be affecting the signaling pathway somewhere upstream of calcium influx [80]. Additional evidence for a mechanism upstream of calcium influx was provided by Pelletier, who found that As does not inhibit compound 48/80-mediated degranulation, suggesting that As does not significantly disrupt phospholipase D activity, protein kinase C function, or the calcium influx process itself [81]. Taken together with Hutchinson's calcium ionophore data, these data strongly suggest that arsenic's effect in RBL cells is upstream of calcium influx and likely involves the phosphorylation events of key signaling molecules, such as Lyn or Syk kinase.

### 1.9. Piceatannol

Piceatannol (3,4,3'5' – tetrahydroxy-*trans*-stilbene) is a secondary natural product isolated from *Euphorbia lagascae* seeds [82]. It has been previously identified as an antileukemic compound and a protein-tyrosine phosphorylation inhibitor [82, 83, 84]. The structure of piceatannol is composed of a stilbene skeleton (a trans ethene double bond flanked by a pair of phenyl group on both carbon atoms of the double bond; Figure 3 A) with hydroxide substituents found on carbons 3, 3', 4 and 5' that have a vital role on its activity [81]. Using a β-hexosaminidase degranulation assay, similar to the one used in our lab (described in "Methods" section), Matsuda *et al* found that not only is piceatannol's α-β double bond (Refer to Figure 3-A) important for activity, but the position of the oxygen-containing constituents is essential for the potency of inhibition [84]. Furthermore, this group found that substituting methoxyl groups in positions 3, 5', and 4' while keeping a hydroxyl group on position 3' increased the inhibitory activity of piceatannol by nearly 12-fold [84].

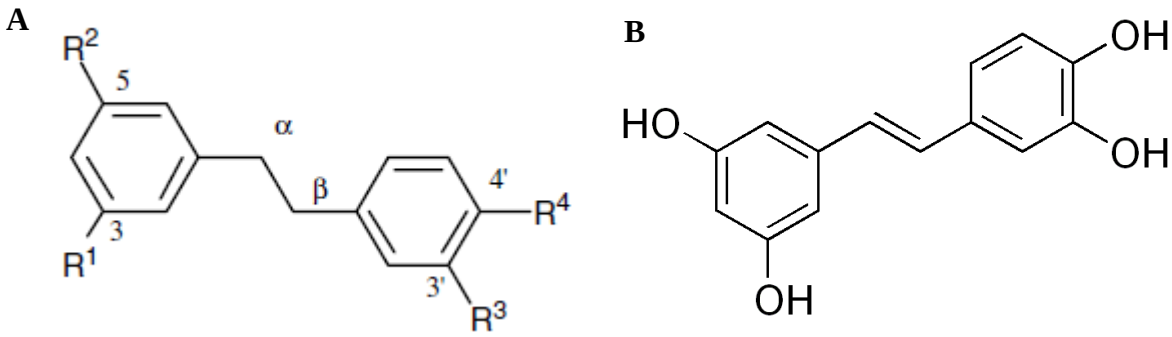


**Figure 3: Structure of Stilbene Skeleton and Piceatannol**

(A) Structure of substituted stilbene skeleton showing the α-β bond and the positions of substituents. (B) Structure of piceatannol. Sources: (A) Matsuda *et al*, 2004 [ref] (B) Sigma-Aldrich Corportation.

Piceatannol's mechanism of inhibition is still debated, but studies have shown it to be a competitive inhibitor of protein-tyrosine kinase activity [82, 83, 85]. In one early study, piceatannol isolates were incubated with p40, a protein-tyrosine kinase, and the catalytic subunit of cAMP-dependent protein kinase to measure its effect on enzyme activity. The study found that piceatannol competed with angiotensin 1 (a tyrosine-containing peptide) for the substrate binding site of p40, but did not compete with the substrate for the catalytic subunit of cAMP-dependent protein-serine kinase, a peptide composed of Leu-Arg-Arg-Ala-Ser-Leu-Gly [82]. Geahlen *et al* concluded that piceatannol selectively inhibits protein-tyrosine kinases by competing for the substrate binding site through a structural resemblance to the tyrosine residue located on the substrate, which lended some insight into future studies involving Syk and other protein tyrosine kinases [82]. Years later after the discovery of Syk (also known as $p72^{syk}$), Oliver *et al* released a study describing piceatannol as a direct inhibitor of the PTK Syk [83]. In this study they first found that both Lyn and Syk were inhibited by piceatannol; however, the difference between the IC50 for Syk and Lyn was approximately 10-fold with Syk being inhibited most readily [83]. Through the use of an anti-Tyr immunoprecipitation assay, this study also concluded that a pretreatment with piceatannol inhibited the tyrosine phosphorylation of Syk in a dose-dependent manner. Oliver *et al* also carried out a similar study using whole RBL-2H3 cells and found similar results. Additionally, these whole cell studies found that the PTK phosphorylation was maximal within 1-2 min of antigen stimulation, the inhibition by piceatannol occurred only upstream of calcium influx, and piceatannol did not inhibit the antigen-stimulated

phosphorylation of the receptor β and γ subunits. Finally, Oliver *et al* elegantly showed that piceatannol prevented antigen-induced ruffling and spreading (events often coupled to antigen stimulation of mast cells; [83]), which replicated the results of a previous study by Pfeiffer *et al* [86].

Herein, we will attempt to elucidate if there is a relationship between the arsenic inhibition and the piceatannol inhibition of mast cell degranulation using a combination experiment. These combination experiments will provide us with more evidence as to whether Syk is the protein responsible for the arsenic inhibition.

## 2. Materials and Methods

### 2.1. Cell Culture

All experiments were carried out using Rat Basophilic Leukemia clone 2H3 (RBL-2H3) cells. These cells were chosen due to their robust degranulation capabilities and their constituent expression of FcεRI –IgE receptors (See "Introduction"). The RBL-2H3 were obtained as a gift from D. Holowka (Cornell University, Ithaca, NY, USA). These cells were maintained in a monolayer culture within sterile, tissue culture treated polystyrene flasks. Great care was taken to avoid plastics known to be possible sources of endocrine disrupting chemicals (i.e bisphenol A, polyvinyl chloride, polydimethylsiloxane, polyethylene terephthalate). While in culture, the cells were kept immersed in Eagle's minimal essential media (EMEM, with EBSS and L-Glutamine; BioWhittaker Lonza) with 20% fetal bovine serum (FBS; Premium grade; Atlanta Biologicals) and 10 µg/mL gentamicin sulfate (BioWhittaker Lonza) to protect the cells

from infection. The culture conditions consisted of a constant temperature of 37°C and levels of $CO_2$ of 5% within a NAPCO Series 8000 WJ $CO_2$ incubator (Thermo Scientific). Flasks of cells were passed on a weekly basis using trypsin (0.05% porcine trypsin with EDTA in HBSS; HyClone Laboratories Inc.), for up to three months. At around 20 completed passages or upon the observation of undesired cell function due to acquired genetic mutations (gross morphological changes, major swings in degranulation capacity or other phenotypic changes), a new vial of cryogenically frozen RBLs was thawed and the previous cell stock properly discarded. To prevent a mycoplasma infection, all materials coming in contact with cell culture were sterilized using 70% ethanol solution and all cell culture passages were carried out within a SteriGARD (The Baker Company) tissue culture hood periodically cleaned with 70% ethanol. Additionally, all buffers were sterile-filtered using Zap Cap filters (0.2 mm filter; PALL corporation) and a mycoplasma detection test was performed monthly using the MycoAlert mycoplasma detection kit (Lonza).

## 2.2. Reagents and buffers

### 2.2.1. Arsenic Stock Preparation

Arsenic (As) for all experiments was prepared by Lee Hutchinson on 4/30/2011, as described in his thesis (Hutchinson Thesis, 2011). These stocks were concluded to be stable because data previously published was successfully replicated with these stocks (see "Results" section.) As described in Hutchinson's graduate thesis: "Arsenic (As) for all experiments was prepared under sterile conditions as 10 mM stocks of inorganic sodium meta-arsenite (+3 oxidation state) (Baker Analyzed, 98.0% minimum, NaAsO2,

CAS # 7784-46-5; JT Baker), and dissolved in cell culture water (sterile, reverse osmosis, deionized, distilled Water for Cell Culture Applications; BioWhittaker Lonza). It was next filtered with a 0.2 m syringe filter for sterility, aliquoted into sterile polypropylene microfuge tubes, and frozen at -20°C until day of use. No stocks were re-frozen after initial thawing for any experiment" [84].

### 2.2.2. Piceatannol Stock Preparation

Piceatannol (EMD Milipore) powder was purchased as 1mg vials and dissolved in freshly made Tyrodes buffer. The solubility of piceatannol in water-based buffers is 0.5 mg/mL and 10 mg/mL in DMSO and Ethanol. Piceatannol was dissolved in the water-based Tyrode's buffer in an effort to prevent known interference effects from the DMSO and ethanol. Due to its low solubility in water, however, great care was taken to ensure the piceatannol was fully dissolved within the buffer. Furthermore, all experiments using piceatannol included a NanoDrop Spectrophotometer (ND-1000; NanoDrop Technologies) UV-Vis analysis prior to use in order to obtain the most accurate concentration measurement. To calculate the concentration of piceatannol, a 0.1 mm path length was used and the absorbance at 320nm was noted. The molar extinction coefficient of piceatannol was calculated to be 0.045 $\mu M^{-1}$ $cm^{-1}$ from the data published by Li *et al* [87]. These stocks were frozen at -20 °C until the day of use. Manufacturer's instructions of storage included storing the piceatannol stock under argon or likewise at -80°C. For convenience, the piceatannol stocks were made immediately before use and discarded.

### 2.2.3. Tyrode's Buffer Preparation

Tyrode's buffer was used as the vehicle for piceatannol and Bovine Serum Albumin (BSA; Calbiochem) vehicle. It was extensively used throughout all experiments, so stocks of 1L were made and stored at a temperature of 4°C. This buffer contained 135 mM NaCl (BioUltra; Sigma-Aldrich), 1.8mM $CaCl_2$ (dihydrate; ACROS organics), 5mM KCl (JT Baker), 1mM $MgCl_2$ (hexahydrate; BDH), 5.6 mM D-(+)-glucose (anhydrous; MP Biomedicals) and 20mM HEPES sodium salt (Ultra-pure; JT Baker). Stocks of NaCl, $CaCl_2$, KCl, and $MgCl_2$ were made to concentrations of 0.5 M or 1M and kept at 4°C for multiple preparations of the buffer. These stocks were dissolved using MiliQ ultra-pure water (Milipore) and sterilized through a bottle-top filter (Corning). The buffer was prepared through the combination of ingredients to their exact corresponding concentration, diluted using MiliQ water, and sterilized using ZapCap 0.2mm filters. The pH of the buffer was adjusted to 7.4 using concentrated HCl (12N; BDH Aristar).

### 2.3. Degranulation Assay

To quantify the extent of degranulation of RBL-2H3 following treatment, we used a β-hexosaminidase activity assay. The enzyme β-hexosaminidase (β-hex) is a natural product of degranulation and is released into the supernatant of culture cells. A synthetic substrate of β-hex, 4-methylumbelliferyl-*N*-acetyl-D-glucosaminide (Calbiochem), is cleaved to produce the fluorescent compound methylumbelliferrone that allows for a direct measure of degranulation [35]. A fluorescent microplate reader (BioTek Synergy 2) was used in accordance to a previous assay as described by Naal *et al* [35].

For every degranulation experiment, RBL cells were harvested 2-4 days after passage using a 5 min. (37°C) trypsinization treatment to dislodge the cells. Following an

8 min centrifugation at 500 *g*, the cells were resuspended at a density of 0.5 x $10^6$ cells/ mL in fresh media. The cells were then plated in a black flat-bottom, tissue-culture treated, sterile 96-well plate (Greiner Bio-One) at a volume 100 µL per well. There additions were randomized to minimize systematic error. Finally, the plate was incubated overnight (12-16 hr.) at 5% $CO_2$ and 37°C.

All degranulation experiments herein included the following treatments in triplicates following IgE sensitization (discussed below). The addition of these treatments was randomized and plates were flipped accordingly to eliminate plate position effects. Each plate contained: (1) Antigen stimulation wells via DNP-BSA; (2) Spontaneous release via Tyrodes-BSA (at 1 mg/mL BSA) buffer ; (3) Total β-hex release via Triton- X 100 (Surfact-Amps X-100, 10%, low carbonyl and peroxide; Thermo Scientific) detergent cell lysis; (4) Background control wells with Tyrodes-BSA buffer and no cells.

Upon completion of the overnight incubation the spent media was discarded and replaced with 100µL fresh media containing 0.1 µg/mL of anti-dinitrophenyl (DNP) mouse IgE (monoclonal, clone SPE-7; Sigma-Aldrich). The plate was incubated for 1 hour at 37°C and 5% $CO_2$ to allow for sensitization of the IgE receptors. After the IgE sensitization, the media mixture was discarded and the plate was washed twice with Tyrodes-BSA buffer (BT) to remove any IgE-media remnants.

Antigen treatments were solutions containing Tyrodes-BSA and multivalent DNP-BSA at the appropriate concentration. DNP-BSA antigen is BSA that has been conjugated with an average of 15 dinitrophenol (DNP) groups. The DNP- BSA was prepared as described by Hardy *et* al [88] and donated by D. Holowka and B. Baird at

Cornell University. Wells containing cells to be stimulated received 200 µL of the appropriate concentration of DNP-BSA antigen (concentrations varied depending on the experiment). Wells designated as spontaneous received 200 µL of BT and those designated as "total release" were exposed to 0.2% Triton at a volume of 200 µL. Wells designated as background received 200 µL of BT and were used to measure background fluorescence. After finalizing all additions, the plate was incubated in a cell incubator at 5% $CO_2$ and 37°C for 1 hour.

After the 1 hour treatment, plates were placed on ice to halt degranulation. A sample of 25 µL was removed from each treated well and combined with 100 µL of 1.2 mM β-hex substrate (4-methylumbelliferyl-N-acetyl-β-D-glucosaminide; dissolved in acetate buffer) in a fresh, pre-cooled 96 well plate. The acetate buffer used to dissolve the β-hex contains acetic acid (glacial, ACS and USP grade; BDH Aristar) at a concentration of 0.12 M titrated to a pH of 4.4 with sodium hydroxide (10N; JT Baker). The fresh plate containing the substrate and supernatants was incubated for 30 min at 37°C. At 30 min the reaction in the wells was quenched by adding 200 µL of cold glycine-carbonate buffer. The glycine-carbonate buffer contained 0.356 M glycine (Omnipur; EMD) and 0.444 M sodium carbonate (anhydrous, granular, ACS grade) titrated to pH of 10.

Following the 30 min incubation of the enzyme and the substrate we used a microplate reader (Synergy 2; Biotek) to measure the activity of β-hex. The hydrolyzed substate was excited using a 360/40 nm excitation filter and the fluorescence intensity was read using 460/40 nm emission filter at normal speed and with a sensitivity setting of 40. Other settings included a distance of 7mm top optical offset and top 50% optics

position. The raw data was processed by first subtracting the background fluorescence value corresponding to wells with only BT. Second, the corrected values were divided by the average total release (average raw fluorescence values of Triton-X 100 cell supernatants) to yield a percent degranulation value.

Experiments using piceatannol included an extra step following IgE sensitization but preceding antigen stimulation as described by Naal *et al* [35]. The piceatannol step was a 10 minute exposure to 100 µL/well of varying piceatannol concentrations added immediately after two BT washes. After the 10 minute incubation the piceatannol treatment was discarded and the addition of $1 \times 10^{-3}$ µg/mL DNP-BSA antigen followed. Appropriate piceatannol-BT and piceatannol-Spontaneous controls were used for the calculations of piceatannol containing treatments. These controls were necessary, because piceatannol was shown to have some effect on both background fluorescence and spontaneous release (See Results Section for more information).

Experiments using arsenic included a modification of the antigen addition step. Arsenic was added into the antigen mixture prior to the addition to the plate. For the wells not receiving arsenic, water (As vehicle) for cell culture (ultrafiltered, reverse osmosis, deonized, distilled; Lonza) was added. After the addition of arsenic, or cell water, to the antigen treatments, each corresponding well received 200 µL of the appropriate treatment.

### 2.4. Phospho-Syk ELISA

The early results of piceatannol experiments provided some indirect evidence of the involvement of the protein-tyrosine kinase, Syk, in arsenic inhibition of degranulation

(See “Results” and “Discussion” sections for more information). With support from the literature about arsenic disrupting phosphorylation patterns, we decided to seek a more focused analysis of the phosphorylation of Syk under various treatments. After looking through our options, we decided upon a Sandwich Phospho-Syk ELISA (Figure 4).

An ELISA, Enzyme-Linked Immunosorbent Assay, is a common biochemical method used to screen for a specific antibody or to quantify an antigen in a sample [89]. There exist many variations including indirect, direct competitive, antibody-sandwich, double antibody-sandwich, direct cellular, and indirect cellular ELISAs. Herein we will describe the protocol of the ELISA used in our experiments, an antibody-sandwich ELISA; for a description of the other types please see Hornbeck *et al* as referenced here [90]. An antibody-sandwich ELISA is often regarded as the most sensitive ELISA available with detection measurements between 2 and 5 times higher than the other types [90]. A typical antibody-sandwich ELISA consists of a 96-well plate coated with a capture antibody specific for the antigen in question. The wells are incubated with a test solution containing the antigen (often a whole cell lysate or a blood sample) and washed to remove unbound antigen. Later, a detection antibody conjugated to enzyme is added, which binds to the antigen in question and acts as a developing agent in later steps. The wells are once more washed to remove any unbound detection antibody and the addition of the enzyme substrate is added. This substrate is hydrolyzed by the enzyme bound to the detection antibody, which either fluoresces upon stimulation (fluorescent) or produces a color that can be measured via absorption (chromogenic). Due to the 1:1 binding, the extent of substrate hydrolysis as measured by a plate reader is proportional to the amount of antigen present in the original sample [90].

The PathScan® Phosho-Syk (panTyr) sandwich ELISA used in our experiments was acquired from Cell Signaling Technologies (CST) as a kit. This ELISA was manufactured to detect endogenous levels of phosphorylated Syk and included all necessary materials for the ELISA protocol; it is a chromogenic ELISA. The kit included a Syk antibody coated 96-well plate, separated into twelve 8-well strips for individual experiments, the biotinylated phospho-tyrosine mouse detection antibody (primary detection antibody specific for phosphor-tyrosine Syk), the HRP-linked streptavidin (enzyme conjugated secondary antibody specific for the primary antibody), the TMB substrate (HRP substrate), a proprietary STOP solution, a 20X wash buffer, a proprietary sample diluent, a 10X cell lysis buffer (containing 20mM Tris (pH 7.5), 150mM NaCl, 1mM EDTA, 1mM EGTA, 1% Triton X-100 [lysing detergent], 2.5mM sodium pyrophosphate, 1mM β-glycerophosphate, 1mM $Na_3VO_4$, 1µg/mL leupeptin) and sealing tape to prevent vaporization during incubation times. The kit was instructed to be stored at 4°C with the exception of the 10X cell lysis, which was instructed to be stored under -20°C.

The protocol that will follow is a modified version of the CST provided protocol. The lysates were extracted from whole RBL-2H3 cells passed and cared for as described above in the "Cell Culture" section. RBL cells were harvested 3-6 days after passage using a 5 min. (37°C) trypsinization treatment to dislodge the cells. Following an 8 min centrifugation at 500xg, the cells were resuspended at a density of $1.75 \times 10^6$ cells/ mL in fresh media. The cells were then plated on 10cm tissue-culture treated, sterile dishes (Cellstar, Acquired from VWR International) at a volume of 5 mL per well (final cell

density of $8.75x10^6$ cells per dish). Finally, the dishes were incubated overnight (12-16 hr.) at 5% $CO_2$ and 37°C.

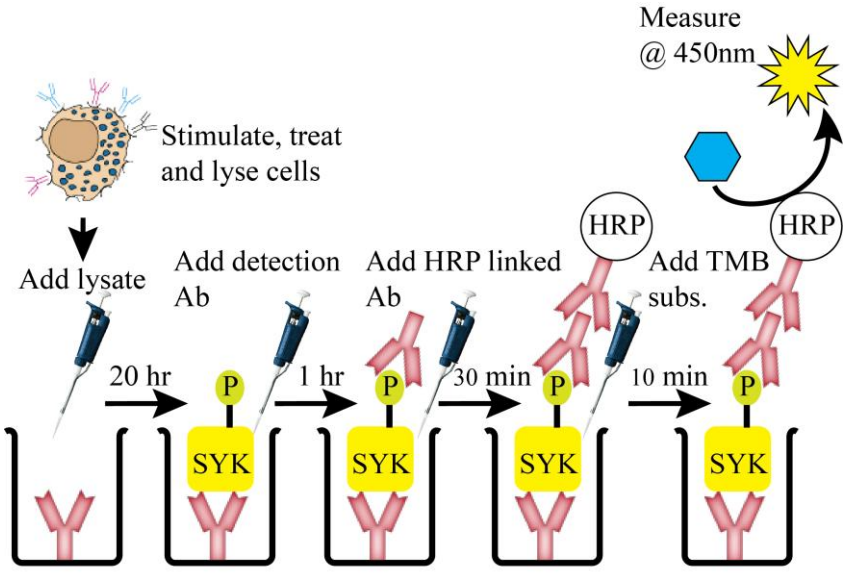


**Figure 4: Summary of ELISA protocol**

Schematic of Phospho-Syk ELISA protocol used herein. Created using Adobe Illustrator CS5

Following the overnight incubation, each dish was checked to ensure a cell confluence between 80 and 90%. The cell media was then immediately discarded and replaced with fresh media containing anti-DNP IgE (Sigma) at a final concentration of 0.1 µg/mL. The dishes were incubated for 1hr at 5% $CO_2$ and 37°C. After the 1hr IgE-sensitization, the spent IgE-media mixture was discarded and washed twice with 5 mL of BSA-Tyrodes to remove any unbound IgE. The 5 mL treatements added next included either BSA-Tyrodes for the unstimulated controls or DNP-BSA antigen at 1µg/mL for stimulated samples. The dishes were incubated for either 5 mins in a bacterial incubator

at 37°C. Immediately after the incubation, the dishes were removed, placed on ice, washed once with ice-cold PBS (4-5mL) and lysed with 0.5 mL of ice-cold 1X lysis buffer containing PMSF for 5 min. The 10X lysis buffer provided in the kit was thawed at 25°C and diluted with purified Mili-Q water before use; Phenylmethanesulfonyl fluoride solution (PMSF; 100mM stock dissolved in Ethanol; Sigma-Aldrich) was added at a concentration of 1mM immediately prior to lysis buffer addition. Following the lysis incubation the cells were harvested into pre-cooled 2 mL microcentrifuge tubes by using a sterile cell scrapper. Each lysate was then sonicated on ice by introducing a clean sonicating probe directly into the lysate. The sonicator was set at 35 watt output and each lysate was sonicated 2 times for 5 sec each time with a 10 sec break in between. Finally, the sonicated lysates were spun down at 14,000 x rpm for 10 min at 4°C. A volume of 100 µL of the clear supernatants from the centrifuged samples were separated from their pellets and placed in new pre-cooled tubes containing 100 µL sample diluent (provided in the CST kit). After a brief vortex, 100 µL of the diluted sample were placed in their appropriate ELISA wells, sealed with tape and incubated overnight (16-20 hrs) at 4°C.

The following day, the plate contents were discarded and each well was washed with 4 times with 200 µL of 1X wash buffer (20X wash buffer provided by CST was diluted using purified Mili-Q water). The washes were followed by an addition of 100 µL of the biotinylated phospho-tyrosine mouse detection antibody to each well. The plate was sealed and incubated at 37°C for 1hr. Following the incubation the well contents were discarded and each well was washed 4 times with 200 µL of 1X wash buffer. Next, 100 µL of the HRP-linked secondary antibody were added to each well, the plate was sealed, and incubated at 37°C for 30 min. Once more, the contents of each well were

discarded and the wells were washed with 200 µL of 1X wash buffer. A volume of 100 µL of the TMB substrate was added and the plate was sealed and incubated for 10min at 37°C. After this 10 min incubation, and immediately before reading, 100 µL of the STOP solution were added to each well. An initial blue color upon addition of TMB substrate indicated a positive reaction, which then changed to yellow when the STOP solution was added. The plate was immediately placed in a BioTek Synergy 2 microplate reader and the absorbance of each well as measured at 450 nm.

Experiments using arsenic included a modification of the antigen addition step. Arsenic was added into the antigen mixture prior to the addition to the dishes. For the dishes wells not receiving arsenic, water (As vehicle) for cell culture (ultrafiltered, reverse osmosis, deonized, distilled; Lonza) was added. After the addition of arsenic, or cell water, to the antigen treatments, each corresponding dishes received 5mL of the appropriate treatment as described in the manufacturer's ELISA protocol.

## 3. Results

### 3.1. Establishment of 1 hr Piceatannol-Arsenic Combination Assay

The piceatannol-arsenic combination assays followed the same structure as the arsenic experiments for which data has been previously published [79] with the exception of the addition of a 10 min piceatannol addition step prior to antigen stimulation [35]. In order to observe a possible effect of this extra step on normal mast cell degranulation (monitored via antigen dose response experiments) we carried out an antigen dose response with a 10 min mock piceatannol step. This mock-piceatannol step was a 10

minute exposure to 100 µL of warmed Tyrode's Buffer added immediately after two BT washes. After the 10 minute incubation the mock-piceatannol treatment was discarded and the addition of various antigen concentrations followed. Appropriate Tyrode's-BT and Tyrode's-Spontaneous controls were used for the calculations of piceatannol containing treatments. The mock-piceatannol antigen dose response (Figure 5-A) elicited a maximal degranulation (at 0.1 µg/mL DNP-BSA antigen) of 41.16% - 46.46% (95% CL) and spontaneous levels of 2.3% ± 0.4 (SD), while a typical antigen dose response (without the extra 10 min pre-stimulation exposure; Figure 5-B) elicited a maximal degranulation (at 0.1 µg/mL DNP-BSA antigen) of 35.61% - 37.93% (95% CL) and spontaneous levels of 1.4 % ± 0.4 (SD). From these results we concluded that the addition of the additional 10 min exposure could be having an effect on the degranulation of RBLs, however, this data represents only a pair of separate experiments so conclusions must be made carefully. Furthermore, the maximal degranulation for the experiment including the mock and the one without (41% and 38%) are similar enough as to conclude that if there is an effect due to this extra step, then it is a small and will likely be abolished by implementing the corresponding controls. It needs to be noted that experiments with cell culture will inherently have variation from experiment to experiment depending on the number of passages that have been carried out on a particular thaw, the day the cells are harvested, and the time the cells spend in culture (unpublished observations).

Previously published data from this lab revealed that lower concentrations of antigen yielded the strongest arsenic dampening effect [79]. Keeping this in mind, we carried out several experiments involving a 10 min piceatannol mock step prior to

stimulation with (A) 0.00002 µg/mL, (B) 0.00004 µg/mL, and (C) 0.001 µg/mL DNP-BSA antigen (Figure 6). Each experiment also received varying arsenic concentrations. Low concentrations of antigen with the 10 min mock piceatannol step resulted in unreliable and highly variable results, likely due to the low extent of degranulation observed (less than 3% degranulation). The maximal degranulation for the lower antigen concentrations without arsenic was at, or around, the same level as spontaneous degranulation. A higher antigen concentration (0.001 µg/mL) was thus chosen. The outcome was a replication of the arsenic inhibition pattern observed in the Hutchinson *et al* [79]. In the absence of As, the absolute level of degranulation was 26% ± 3% (SD); untreated cells yielded spontaneous degranulation levels of 3.1% ±0.5 (SD) (Figure 6). This absolute level of degranulation is comparable to the level elicited by 0.0004 µg/mL DNP-BSA in previously published results (Compare 26% ± 3% (SD) observed in Figure 6 to 25% ± 1% (SD) observed in Hutchinson *et al*) [79]. At the highest concentration of arsenic of 750ppb, our experiments showed a ~31% inhibition of degranulation (Figure 6) that is comparable to the ~37% (0.63-fold inhibition) inhibition observed in Hutchinson *et al* for experiments eliciting similar absolute levels of degranulation in the absence of As [79]. These results affirmed the potency of the arsenic stock, and it also enabled us to choose the antigen concentration that that was to be used for all piceatannol experiments.

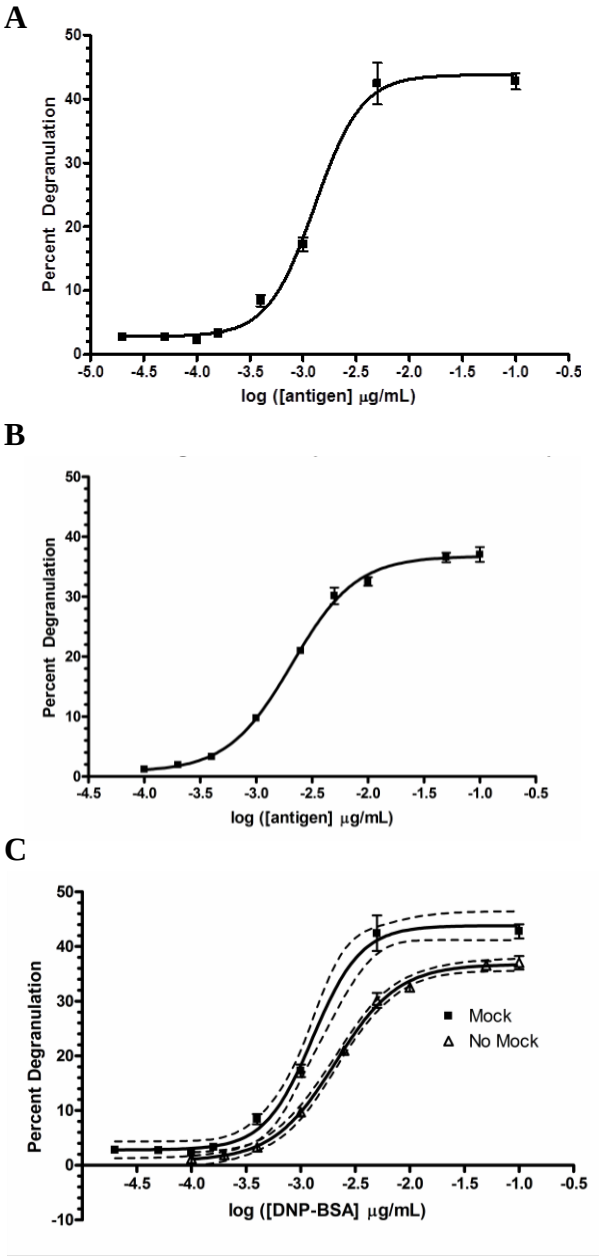


**Figure 5: Effects of 10 min Exposure Step Pre-Stimulation**

RBL cells were cultured overnight and washed twice with Tyrodes-BSA. Cells were either (A) exposed to warm Tyrode's buffer for 10 minutes prior to antigen stimulation or (B) lacked this additional 10 min exposure step. The β-hexosaminidase release (expressed as a percentage of degranulation) is plotted against the $\log_{10}$ [DNP-BSA]. (C) is a combined plot of (A) and (B) with their respective 95% CI as dashed lines. Graphs are expressed as means ± SD; two experiments for each graph; three replicates per dose per experiment. Best fit line plotted was calculated using the "Sigmoidal regression (variable slope)" function in GraphPad Prism version 4.

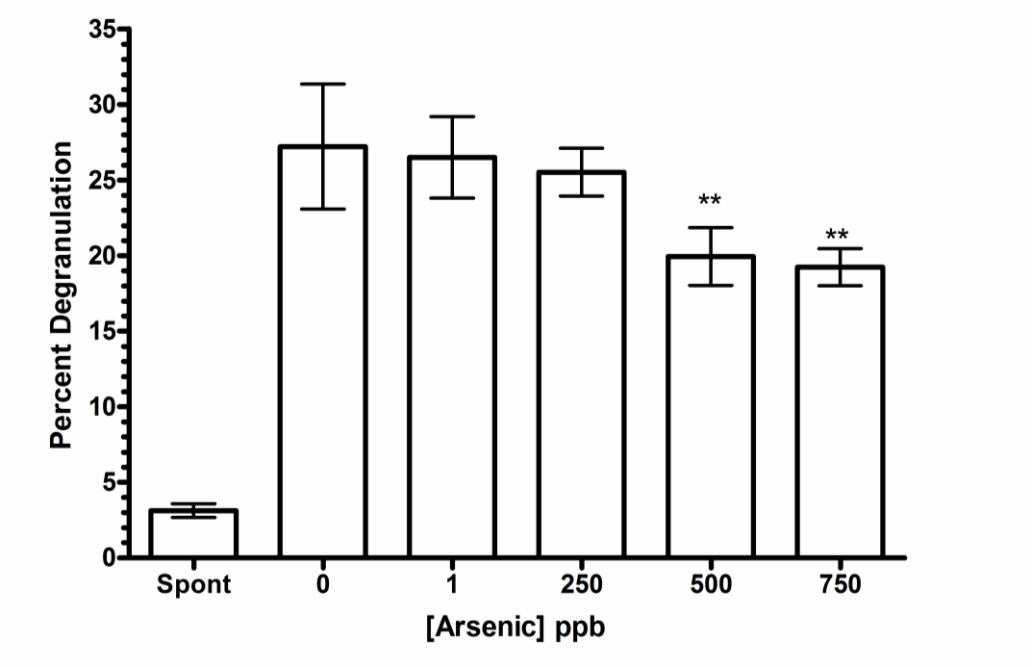


**Figure 6: Optimization of Antigen Concentrations for 1 hr Piceatannol-Arsenic Combination Assays.**
RBL cells were cultured overnight and washed twice with Tyrode's buffer. Cell were then exposed to warm Tyrode's (piceatannol mock) for 10 min prior to stimulation with 0.001 µg/mL DNP-BSA for 1 hr. Each experiment also included a simultaneous exposure to varying doses of arsenic during this 1 hr stimulation period. One way ANOVA tests were implemented and statistical significance when compared to 0 ppb is symbolized as ** for p-values less than 0.001.

### 3.2. Effects of Piceatannol-Arsenic Co-Exposure on 1 hr DNP-BSA Mediated Degranulation

An investigation of the effect of piceatannol-arsenic co-exposure was performed. Using varying doses of piceatannol during a 10 min pre-stimulation exposure as followed by a 1hr antigen ± 750ppb arsenic exposure, it was found that 200 µM piceatannol, in combination with arsenic, dampened degranulation by ~77% while the exposure to arsenic alone produced a ~23% inhibition of degranulation (Figure 7). In the absence of arsenic and piceatannol, these experiments elicited an absolute level of degranulation of 35.2% ± 3% (SD) and spontaneous levels of 5.2% ± 0.7% (SD). This absolute level of degranulation is comparable to the level elicited by 0.0004 µg/mL DNP-BSA in

previously published results (Compare 35.2% ± 3% (SD) observed in Figure 7 to 25% ± 1% (SD) observed in Hutchinson *et al*) [79]. These results also fall in line with previous data shown in this report of 26% ± 3% (SD) (Figure 6). At the highest concentration of arsenic of 750ppb without piceatannol, our experiments showed an average of ~24% inhibition of degranulation that is comparable to the ~37% (0.63-fold inhibition) inhibition observed in Hutchinson *et al* [79] and ~31% reported earlier in this thesis (Figure 6) for experiments eliciting similar absolute levels of degranulation. The arsenic inhibition of degranulation was consistent throughout the doses 0 μM, 20μM, and 100 μM piceatannol (inhibitions were ~26%, ~28%, ~29% respectively), however, at 200 μM piceatannol this inhibition was only ~12% (Calculated based upon the change in inhibition [No As – As] for each piceatannol dose) (Figure 7). In the absence of arsenic, the piceatannol inhibition of degranulation for doses 20μM, 100 μM, and 200 μM was ~13%, ~37%, and ~65% respectively (Figure 7). Co-exposure to 750 ppb arsenic and 20μM, 100 μM, and 200 μM piceatannol inhibited degranulation by ~41%, ~66%, ~77% respectively (Figure 7).

Piceatannol did show some concerning effects on spontaneous degranulation, however. Although insignificant in the combined data, individual spontaneous results showed piceatannol-arsenic co-exposure induced inhibition of up to 10% that should be noted (Figure 8-A). All raw fluorescence values were compared to their respective controls (i.e piceatannol-arsenic exposures were compared to arsenic with no piceatannol background samples; piceatannol only exposures were compared to no arsenic-no piceatannol background samples) when calculating percent degranulation to avoid any

possible piceatannol induced interference of background fluorescence. Still, it was found piceatannol at 200 µM decreasing background fluorescence by 20% when compared to Tyrode's-BSA sample (Figure 8-B).

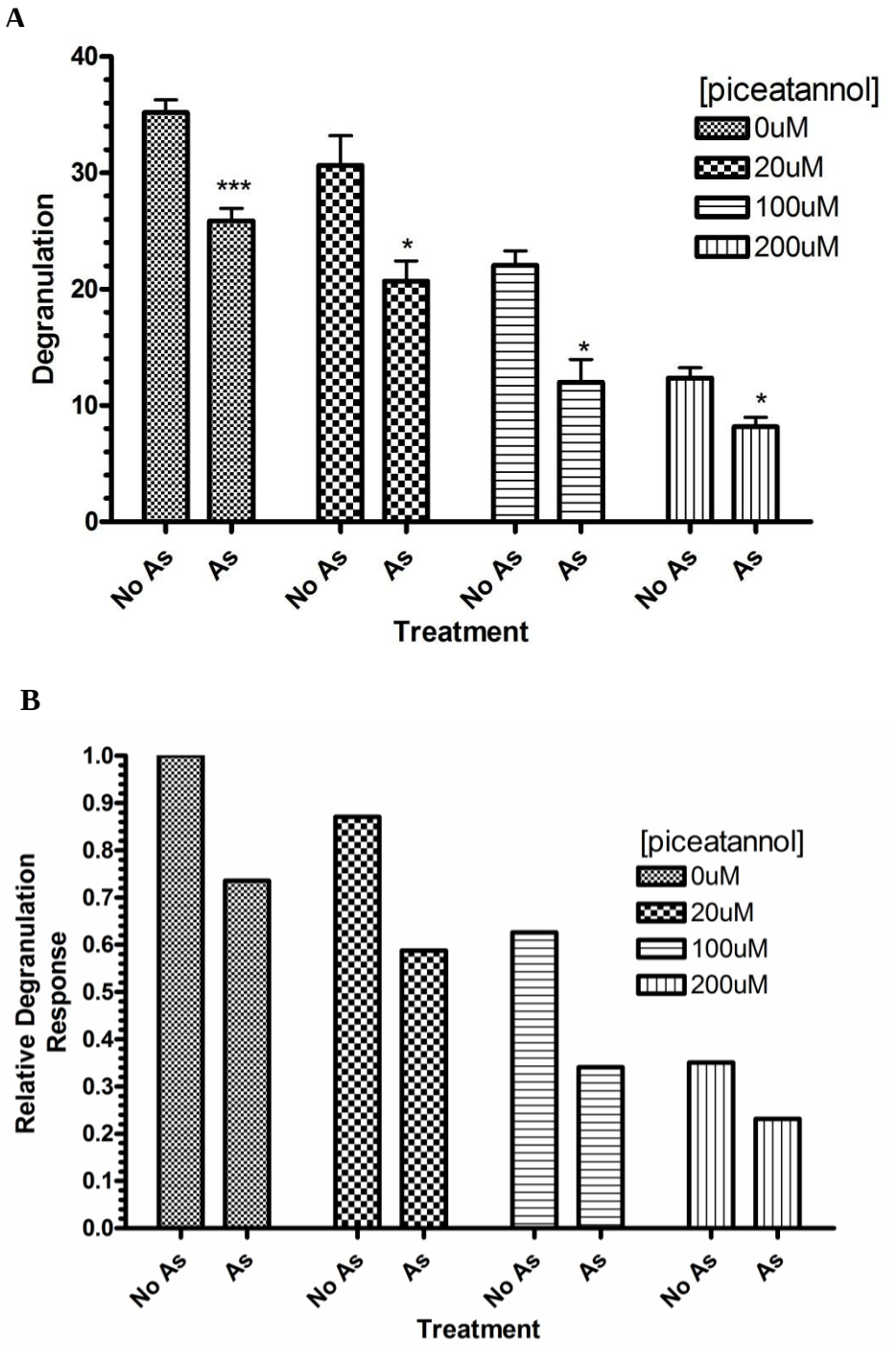


**Figure 7: Effects of Piceatannol-Arsenic Co-Exposure on 1 hr DNP-BSA Mediated Degranulation**

RBL cells were cultured overnight and washed twice with Tyrode's buffer. Cell were then exposed to piceatannol at the indicated doses for 10 min prior to stimulation with 0.001 µg/mL DNP-BSA and simultaneous exposure to 750ppb for 1 hr. (A) Combined data, (B) Normalized data reported in (A): Values were normalized to . In graphs (A) and (B) percent of degranulation is plotted against the concentration of piceatannol. The results of antigen stimulated cells exposed to no arsenic and no piceatannol (No As, 0 uM piceatannol . (A) was evaluated using individual t-tests by comparing the As to No As treatments for each piceatannol concentration. * and *** represent p-values of less than 0.05 and 0.0001 respectively.

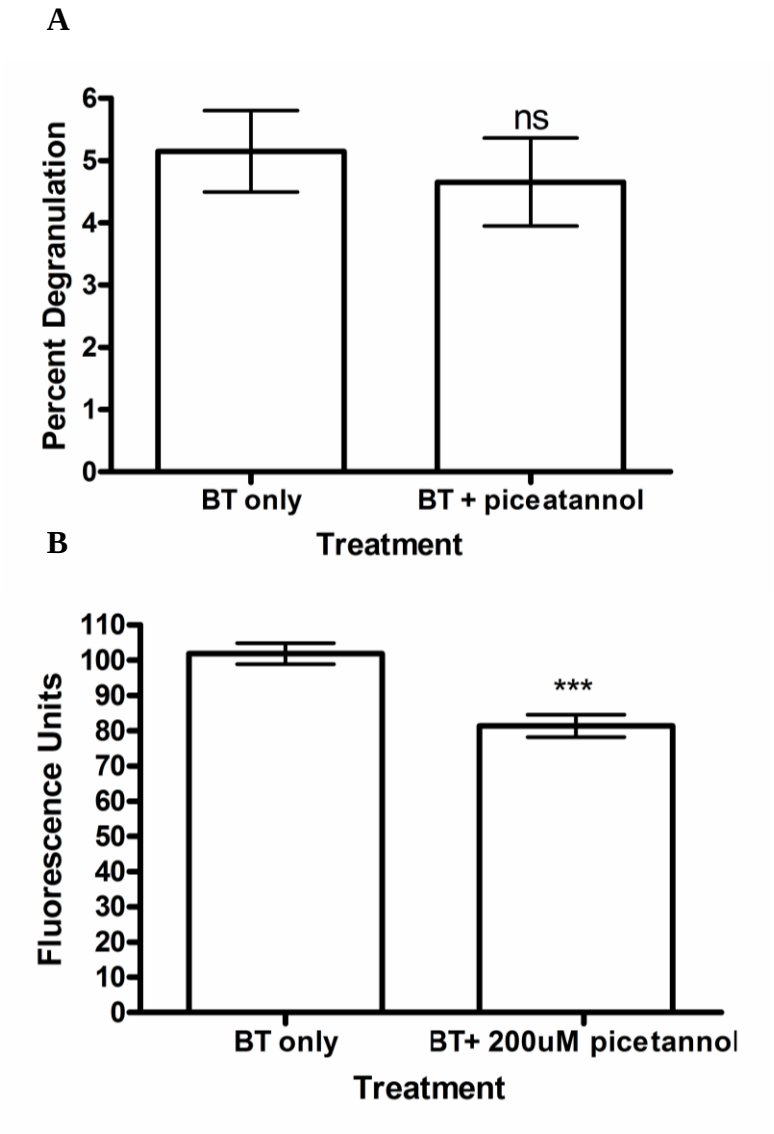


**Figure 8: Effects of 200 µM Piceatannol on Spontaneous Release and Background Fluorescence**
Effects of 200 µM piceatannol on (A): Spontaneous release and (B) Background fluorescence. (A) RBL cells were cultured overnight and washed twice with Tyrode's buffer. Cells were then exposed to piceatannol at the indicated doses for 10 min prior to BSA- Tyrode's addition (as opposed to antigen stimulation). (B) Wells with no plated cells were washed twice with Tyrode's buffer. Wells were then exposed either warm Tyrode's (BT bar) or 200 µM piceatannol for 10 min prior to BSA-Tyrode's exposure for 1hr. Unpaired t-tests were run to evaluate significance: ns= not significant; ***= p-value < 0.0001.

### 3.3. Establishment of Phospho-Syk ELISA Experiments

The protocol for the Phospho-Syk ELISA experiments was heavily based upon the reference protocol provided with the PathScan® Phosho-Syk (panTyr) kit from Cell Signaling Technologies. Still, many individual steps in this protocol had to be tailored to our system (See Figure 9 for all optimizations). The first of these steps was the sonication procedure. Cells were lysed as described in the "Methods" section, scraped off the dishes, and sonicated at 35Watts at different time intervals. The lysates were inspected for live cells and counted under the microscope using trypan blue dye. Ultimately, it was found that sonicating the lysates at 35 Watts 3 times for 5 seconds, with 10 seconds breaks in between, resulted in the fastest sonication procedure to fully lyse the cells (results not shown). Due to the fragility of the phosphorylation state of these proteins, it was crucial to ensure that steps following the stimulation of the cells were carried out as quickly as possible. Another step that was evaluated during the development of the protocol was the correct dilution of the lysates and the incubation time of the STOP solution following the incubation of the TMB substrate. The ELISA kit provided a sample diluent, whose ingredients are proprietary, and recommended a 1:1 dilution of the processed lysate prior to addition to the ELISA plate. Using the procedure described in the "Methods" section, it was found that the 1:1 dilution elicited the most robust percent increase in antigen-stimulated Syk phosphorylation with an average percent increase over control (BT) of 25% for all time points (Figure 10-B). Furthermore, immediate reading of the sample following the addition of STOP (0 min columns; Figure 10 A-C), as compared to later timeframes, showed the highest percent increase in Syk phosphorylation for

undiluted and 1:2 diluted samples with 14.57% ± 0.93% (SD) and 17.17% respectively (Figure 10-A and C).

| Parameter Tested | Experimental Result | Conclusion |
|---|---|---|
| Cell density to be cultured in 10cm dishes that produces 80-90% confluence following overnight incubation | Densities tested:<br>$11.375x10^6$ cells/dish: confluence falls within 80-90%<br>$9.625x10^6$ cells/dish: confluence was lower than 80%<br>$8.75x10^6$ cells/dish: considerably underconfluent | Cells will be cultured at $11.375x10^6$ cells per dish for 16-20 hrs to achieve 80-90%. |
| Extent of lysis following various [detergent] in 5 min lysis buffer incubation without scraping | Tested:<br>0.2% TX: low cell lysis<br>0.5% TX: low cell lysis<br>1% TX: moderate cell lysis | As recommended by CST, 1% TX lysis buffer elicits the highest extent of lysis, however, scraping maybe be needed as there was not enough lysis observed |
| Extent of lysis following various [detergent] in 5 min lysis buffer incubation with scraping | Tested:<br>0.2% TX: low cell lysis; almost undisturbed cell lawn<br>0.5% TX: moderate cell lysis; cells looked stressed and some were lysed<br>1% TX: high cell lysis; small number of viable cells observed | The lysis procedure using a lysis buffer with 1% TX and scraping resulted in the highest extend of lysis |
| Sonication of cell lysates that result in no visible whole cells or cellular fragments | Tested:<br>Sonicated 3 times for 5 sec each @ intensity of 25 W: whole cells obseved<br>Sonicated 3 times for 10 sec each @ intensity of 25 W: whole cells observed<br>Sonicated 3 times for 5 sec @ intensity of 35 W: no whole cells, some fragments<br>Sonicated 3 times for 10 sec @ intensity of 35 W: no whole cells, some fragments | The final sonication procedure was chosen to have an intensity of 35W repeated 3 times for duration of 5 secs each. This was chosen over the similar procedure at 10 sec as no difference was observed between these treatments |
| Extent of dilution of cell lysate (immediate reading following STOP addition) | Tested:<br>Undiluted: 14.5% increase over control<br>1:1 dilution: 23% increase over control<br>1:2 dilution: 17.1% increase over control | Reading immediately following the addition of STOP solution (as recommended by CST), it was found that a 1:1 dilution of lysate with the manufacturer's diluent produced the highest percent increase over control in phospho-Syk |
| Extent of STOP incubation time for 1:1 diluted lysates | Tested:<br>0 min: 23% increase over control<br>5 min: 25% increase over control<br>20 min: 24% increase over control | Samples diluted 1:1 with the manufacturer's diluent produced the same percent increase over control in phosphor-Syk regardless of the extent of STOP incubation time. Immediate reading was chosen as recommended by CST. |

**Figure 9: Optimization of the Phospho-Syk ELISA Protocol**

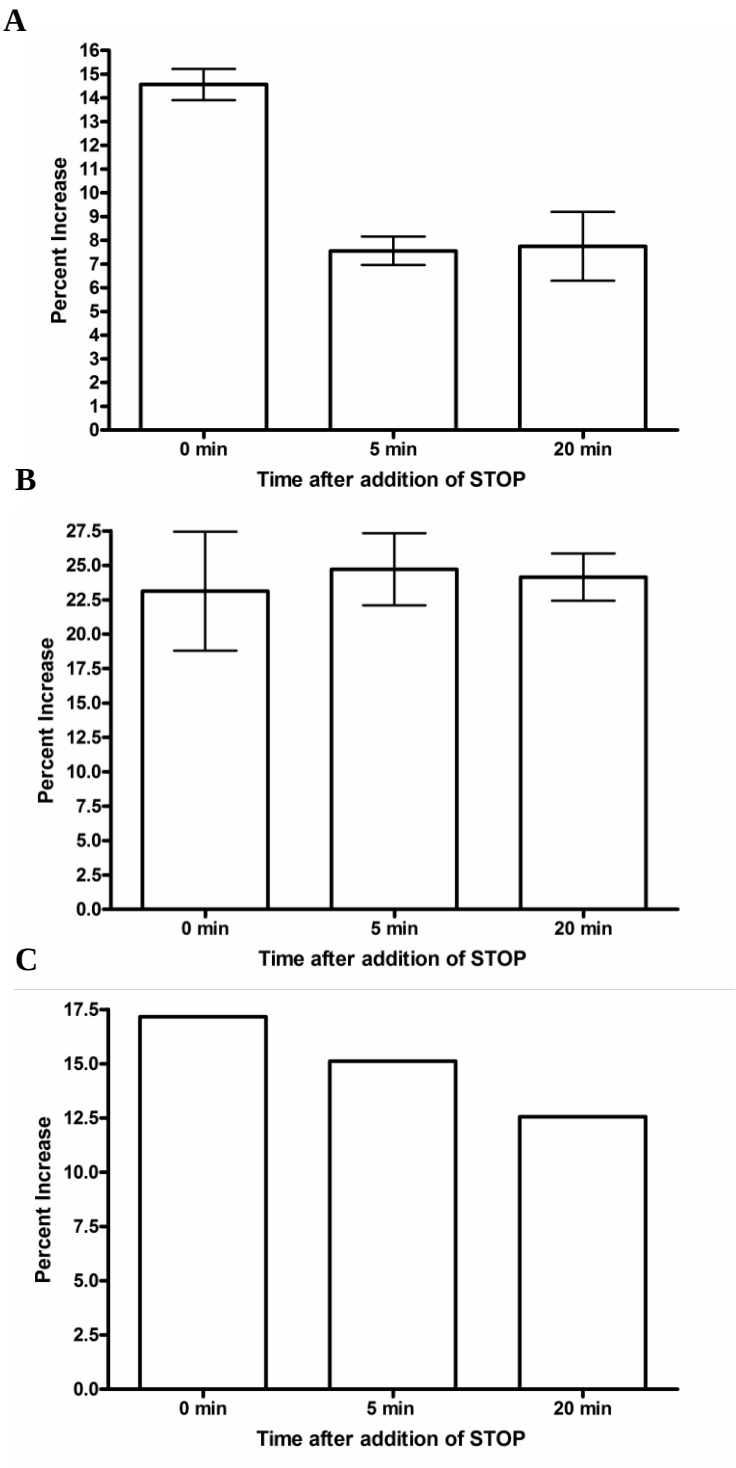


**Figure 10: Investigation of the Effect of Dilution and Incubation Time of the STOP Solution on Phosphor-Syk Phosphorylation as Measured via ELISA.**
Lysate samples were prepared as described in "Methods" Section. Each 100 µL lysate sample was added to the ELISA plate either (A) undiluted, (B) diluted 1:1 with sample diluent, or (C) diluted 1:2 with sample diluent. Samples were plated in duplicates, with the exception of (C) which is only based on one sample; their error bars represent SD.

### 3.4. Investigation of the SYK Gene in Human and Rat

The plates provided with the PathScan® Phosho-Syk (panTyr) kit from Cell Signaling Technologies were coated with anti- human Syk antibodies. Since the cells we used for our experiments were rat cells, we aimed to ensure that there would be appropriate cross-reactivity between the RBL cell' rat Syk and the kit's anti-human antibodies. Thus, we carried out an alignment of the SYK gene in human (*Homo sapiens)* and that of rat (*Rattus norvegicus*). An alignment analysis of the long human isoform SYK and rat SYK in ClustalW2 (http://www.ebi.ac.uk/Tools/msa/clustalw2) using the default settings was carried out and resulted in 91% homology at the protein level and 84% at the nucleotide level (Figures 11 and 12) (Juyoung Shim, unpublished analysis). Such high homology values allowed us to conclude that there is a high probability that anti-human Syk antibodies could in fact recognize rat Syk proteins.

**A**

MASSGMADSANHLPFFFGNITREEAEDYLVQGGMSDGLYLLRQSRNYLGGFALSVAHGRK
AHHYTIERELNGTYAIAGGRTHASPADLCHYHSQESDGLVCLLKKPFNRPQGVQPKTGPF
EDLKENLIREYVKQTWNLQGQALEQAIISQKPQLEKLIATTAHEKMPWFHGKISREESEQ
IVLIGSKTNGKFLIRARDNNGSYALCLLHEGKVLHYRIDKDKTGKLSIPEGKKFDTLWQL
VEHYSYKADGLLRVLTVPCQKIGTQGNVNFGGRPQLPGSHPATWSAGGIISRIKSYSFPK
PGHRKSSPAQGNRQESTVSFNPYEPELAPWAADKGPQREALPMDTEVYESPYADPEEIRP
KEVYLDRKLLTLEDKELGSGNFGTVKKGYYQMKKVVKTVAVKILKNEANDPALKDELLAE
ANVMQQLDNPYIVRMIGICEAESWMLVMEMAELGPLNKYLQQNRHVKDKNIIELVHQVSM
GMKYLEESNFVHRDLAARNVLLVTQHYAKISDFGLSKALRADENYYKAQTHGKWPVKWYA
PECINYYKFSSKSDVWSFGVLMWEAFSYGQKPYRGMKGSEVTAMLEKGERMGCPAGCPRE
MYDLMNLCWTYDVENRPGFAAVELRLRNYYYDVVN\

**B**

MASSGMADSANHLPFFFGNITREEAEDYLVQGGMSDGLYLLRQSRNYLGGFALSVAHGRK
AHHYTIERELNGTYAIAGGRTHASPADLCHYHSQESDGLVCLLKKPFNRPQGVQPKTGPF
EDLKENLIREYVKQTWNLQGQALEQAIISQKPQLEKLIATTAHEKMPWFHGKISREESEQ
IVLIGSKTNGKFLIRARDNNGSYALCLLHEGKVLHYRIDKDKTGKLSIPEGKKFDTLWQL
VEHYSYKADGLLRVLTVPCQKIGTQGNVNFGGRPQLPGSHPASSPAQGNRQESTVSFNPY
EPELAPWAADKGPQREALPMDTEVYESPYADPEEIRPKEVYLDRKLLTLEDKELGSGNFG
TVKKGYYQMKKVVKTVAVKILKNEANDPALKDELLAEANVMQQLDNPYIVRMIGICEAES
WMLVMEMAELGPLNKYLQQNRHVKDKNIIELVHQVSMGMKYLEESNFVHRDLAARNVLLV
TQHYAKISDFGLSKALRADENYYKAQTHGKWPVKWYAPECINYYKFSSKSDVWSFGVLMW
EAFSYGQKPYRGMKGSEVTAMLEKGERMGCPAGCPREMYDLMNLCWTYDVENRPGFAAVE
LRLRNYYYDVVN

**C**

MAGNAVDNANHLTYFFGNITREEAEDYLVQGGMTDGLYLLRQSRNYLGGFALSVAHNRKAHHYTIERELN
GTYAISGGRAHASPADLCHYHSQEPEGLVCLLKKPFNRPPGVQPKTGPFEDLKENLIREYVKQTWNLQGQ
ALEQAIISQKPQLEKLIATTAHEKMPWFHGNISRDESEQTVLIGSKTNGKFLIRARDNNGSFALCLLHEG
KVLHYRIDRDKTGKLSIPEGKKFDTLWQLVEHYSYKPDGLLRVLTVPCQKIGVQMGHPGSSNAHPVTWSP
GGIISRIKSYSFPKPGHKKPPPPQGSRPESTVSFNPYEPTGGAWGPDRGLQREALPMDTEVYESPYADPE
EIRPKEVYLDRKLLTLEDNELGSGNFGTVKKGYYQMKKVVKTVAVKILKNEANDPALKDELLAEANVMQQ
LDNPYIVRMIGICEAESWMLVMEMAAWGPLNKYLQQNRHIKDKNIIELVHQVSMGMKYLEESNFVHRDLA
ARNVLLVTQHYAKISDFGLSKALRADENYYKAQTHGKWPVKWYAPECINYFKFSSKSDVWSFGVLMWEAF
SYGQKPYRGMKGSEVTAMLEKGERMGCPPGCPREMYDLMFLCWTYDVENRPGFAAVELRLRNYYYDVVN

**Figure 11: Raw Nucleotide Sequences of Human and Rat SYK Genes**

(A) |P43405|KSYK_HUMAN Tyrosine-protein kinase SYK OS=Homo sapiens GN=SYK PE=1 SV=1 635aa

(B) |P43405-2|KSYK_HUMAN Isoform Short of Tyrosine-protein kinase SYK OS=Homo sapiens GN=SYK 612aa (Short Isoform)

(C) |NP_036890.1| tyrosine-protein kinase SYK [Rattus norvegicus] 629aa

All sequences were acquired from the National Center for Biotechnology Information (NCBI).

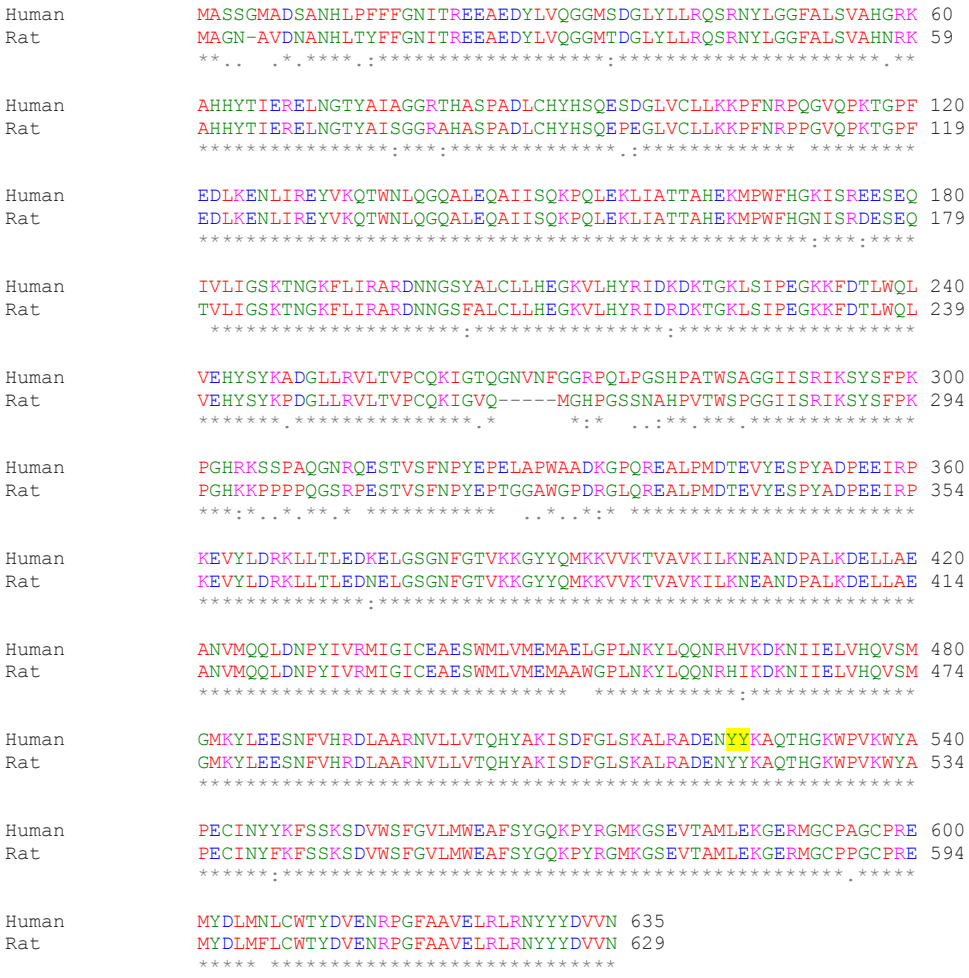


**Figure 12: Alignment of long Human Isoform SYK and rat SYK**

A multiple sequence alignment was carried out using ClustalW2 version 2.1 and the default settings. The yellow highlight is intended to call attention to tyrosine residues 525 and 526 (see Introduction section for more details on these residues).

### 3.5. Effects of 750 ppb Arsenic on Syk Phosphorylation as Measured via Phospho-Syk ELISA

As of the writing of this thesis, the optimization of the ELISA protocol is still a work in progress. Early experiments have had promising results that may point to a pattern of Syk phosphorylation deficiency in the presence of arsenic. An experiment involving monoclonal IgE sensitized RBLs stimulated with 0.001 µg/mL DNP-BSA antigen and treated with 750 ppb arsenic resulted in a pattern of detectable phospho-Syk dampening. As shown in Figure 13A, there is a clear increase in absorbance of antigen-stimulated Syk phosphorylation and then the subsequent decrease likely due to As interference of phosphorylation of Syk. Further processing of the raw absorbance readings demonstrated a clear percent increase in phosphorylated Syk of 30% ± 11% (avg. error; Figure 13 B). When exposed to 750 ppb As, the levels of phosphorylated Syk decreased to 18% ± 5% (avg. error; Figure 13 B), which indicates a decrease of ~42% Syk phosphorylation likely induced by As. However, a one-tailed unpaired t-test carried out with GraphPad Prism showed no statistical significance with a p-value of 0.1801.

As stated earlier, the fragility of phosphorylated proteins requires a swift management and implementation of stimulation and lysis steps. It is these steps that we suspect to be the culprit to the inconsistency in the data and so further optimization of these steps must be carried out before they can produce reliable data. During these optimization experiments, it was proposed that the old arsenic stock could have lost its potency over time (stocks were originally made in 04/30/2011 by Lee Hutchinson). New stocks were thus prepared and their potency was evaluated (Figure 14). At antigen concentrations of 0.0004 µg/mL (Figure 14-A) and 0.00016 µg/mL (Figure 14-B), the maximal

degranulation values (0 ppb As) were 145% ± 1 (SD) and 6.0% ± 0.8% (SD), respectively, and spontaneous degranulation levels of 7% ± 1% (SD). The maximal inhibition elicited by 750 ppb arsenic was ~37% and ~44%, respectively. Spontaneous degranulation was not affected by arsenic (Figure 14-C). These results resemble those published in Hutchinson *et al* by exhibiting a similar dose response inhibition pattern, so the potency of the new arsenic stock was confirmed.

**A**

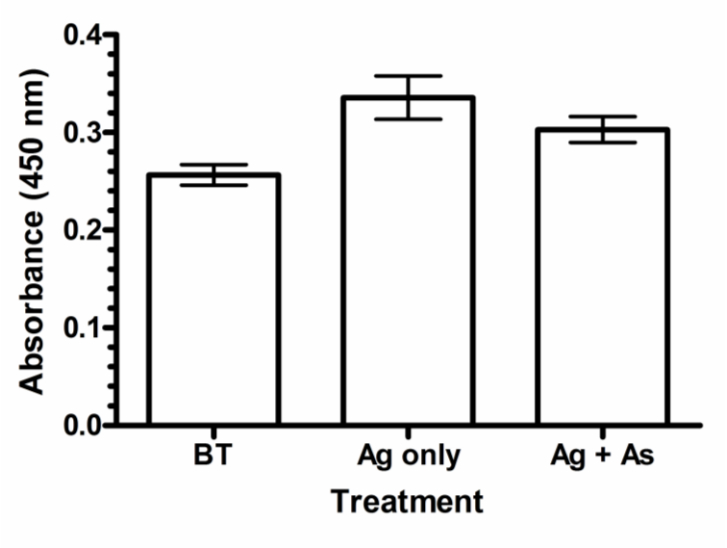


**B**

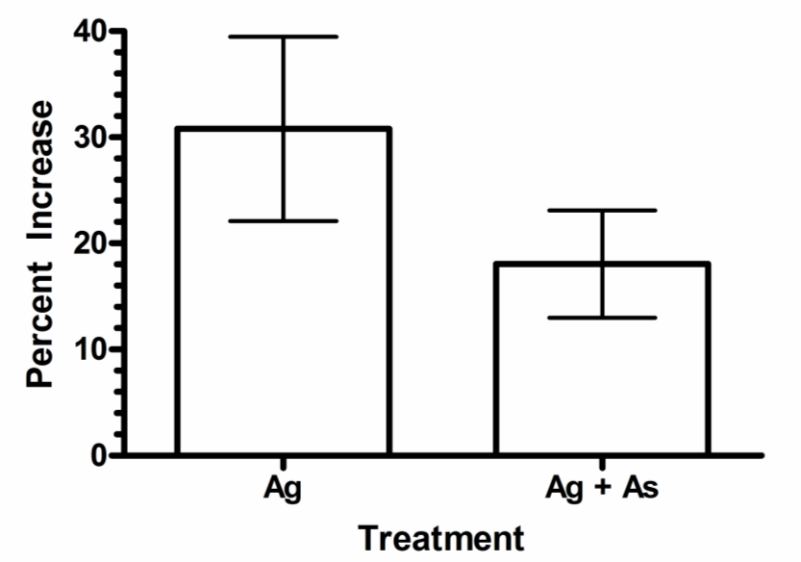


**Figure 13: Effects of 750 ppb Arsenic on Phosphorylated Syk as Measured via Phosho-Syk (panTyr) Sandwich ELISA**

Effects of 750 ppb Arsenic on Phosphorylated Syk as Measured via PathScan® Phosho-Syk (panTyr) sandwich ELISA from Cell Signaling Tech. RBL cells were stimulated with 0.001 µg/mL DNP-BSA antigen and simultaneously treated with 750 ppb As for one hour. Cells were then lysed and diluted 1:1 with sample diluent prior to being added to the ELISA plate. For the complete ELISA protocol see the "Methods" section. (A) Raw absorbance values of Spontaneous (BT; non-stimulated), antigen only, and antigen and arsenic were done in duplicate; Error bars show average error. (B) Percent increase of antigen and antigen & arsenic treatments, over the non-stimulated spontaneous control. (B) is the processed form of the data shown in (A).

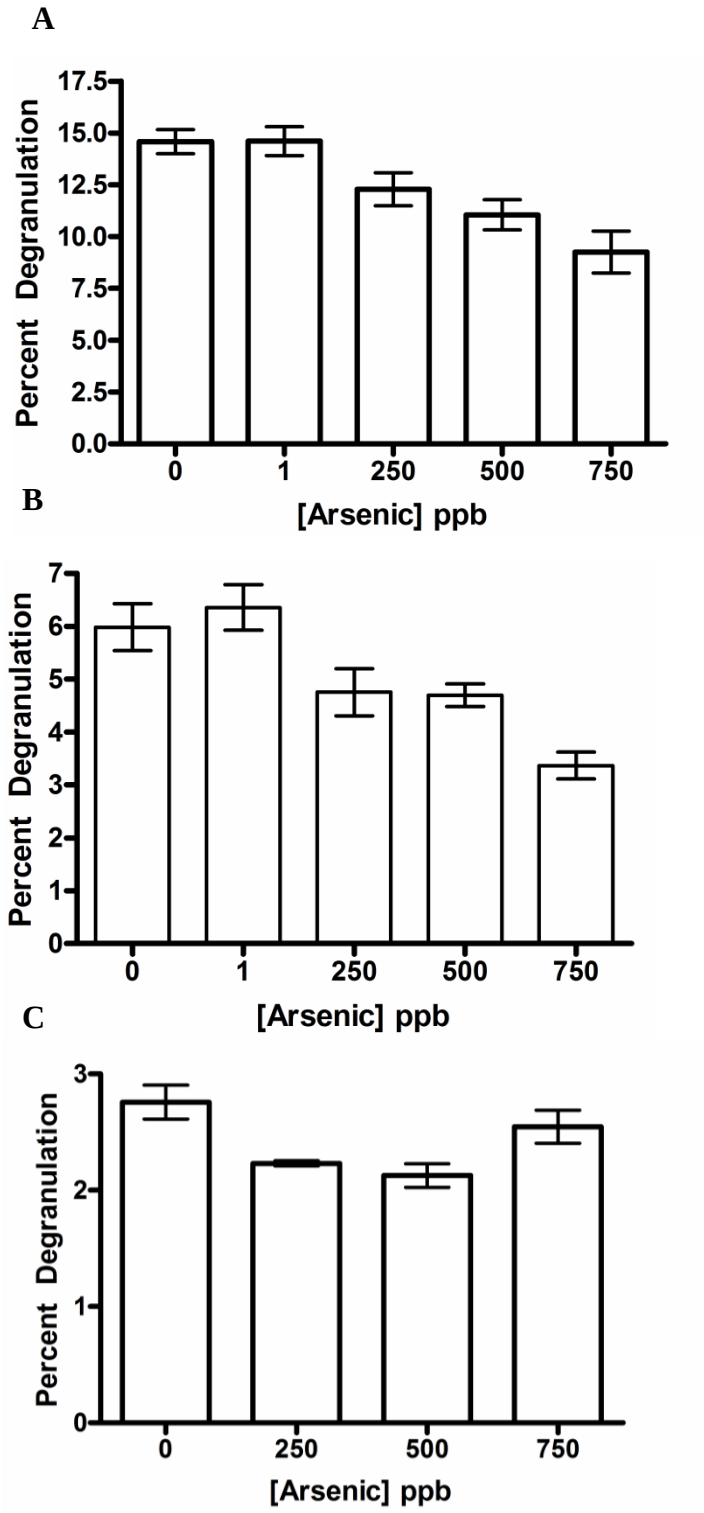


**Figure 14: Investigation of New Arsenic Stock Potency**

RBL cells were cultured overnight and washed twice with Tyrode's buffer. Cells were then stimulated with (A) 0.0004 µg/mL, (B) 0.00016 µg/mL, and (C) Tyrode's buffer (for spontaneous degranulation). Experiments were in done in triplicates; error bars signify ± SD.

# 4. Discussion

## 4.1. Discussion of Piceatannol-Arsenic Co-Exposure on 1 hr DNP-BSA Mediated Degranulation Experiments

While establishing the piceatannol-arsenic combination assay it was found that the additional 10-min step needed to expose the cell to piceatannol could be having an effect on the typical degranulation of RBLs. It must kept in mind that these conclusions were drawn from only two experiments done on different days and using cells that, although were from the same thaw, were not from the same passage. Still, as it is a commended research practice, the controls used to analyze all data included this extra step regardless of whether the effect is real or just an artifact. This meant that spontaneous wells, background wells, and TX-lysis wells all included this additional 10 min piceatannol exposure. Furthermore, the results from the optimization experiments of the antigen concentration, which included the extra 10 min piceatannol mock step, helped to ease our initial concerns. The 0.001 μg/mL concentration of DNP-BSA experiments (Figure 6-C) that exhibited an absolute level of degranulation of 26% ± 3% (SD) in the absence of As showed a comparable inhibition pattern shown in Hutchinson *et al* [79]. Additionally, and more importantly, the maximal inhibition at this concentration (elicited by 750ppb) was comparable to the inhibition elicited by the same exposure to arsenic at 0.0004 μg/mL DNP-BSA antigen. These experiments can be compared, because their absolute levels of degranulation reached a similar degree (compare 26% ± 3% (SD) observed in Figure 6to 25% ± 1% (SD) observed in Hutchinson *et al*) [79]. In that same publication, these experiments with comparable levels of absolute degranulation experienced a maximum

degree of arsenic-induced inhibition of degranulation at 750 ppb with ~37% (0.63-fold) inhibition when compared to its appropriate 0 ppb samples [79]. Likewise, our experiments reported here showed a ~31% inhibition of degranulation (Figure 6) that is comparable to those experiments mentioned above. These results assured us that the potency of our arsenic stock was still at the desired level, and that an antigen concentration of 0.001 μg/mL elicited a level of absolute degranulation for this particular thaw of cells that is comparable to already published data. Furthermore, we concluded then that, by controlling any possible effect of the extra 10 min exposure, we could replicate the previously reported arsenic dose response inhibition of degranulation and thus our piceatannol-arsenic combination assays could be accurately used to investigate the possibility of arsenics involvement in the early tyrosine phosphorylation pathway.

The addition of piceatannol to our arsenic experiments showed a robust and clear inhibition of degranulation. This potent combined inhibition of ~77% at arsenic concentrations of 750 ppb and exposure to 200 μM piceatannol for the piceatannol-arsenic combination assays appears to point to an additive mechanism of inhibition. Exposure to arsenic alone produced an average of ~24% inhibition of degranulation (Figure 7 A andB) while piceatannol, the absence of arsenic, produced a maximal inhibition of degranulation of ~65%. Since only a dose of 750 ppb arsenic was used in these combination experiments, it was expected for arsenic to inhibit all samples equally. This was the case for 3 out of the 4 treatments groups. At 200 μM piceatannol and 750 ppb As, arsenic only attributed ~12% of the inhibition while at all other piceatannol doses the arsenic inhibition remained at constant levels (compare ~12% at 200 μM and 750 ppb

As to ~26%, ~28%, ~29% at 0 µM (and 750 pbb As), 20µM (and 750 ppb As), and 100 µM (and 750 ppb As) piceatannol respectively) (Figure 7). We suspect that the low levels of degranulation of cells treated with 200 µM and 750 ppb As could be help culprit to this erratic behavior. Cells exposed to this treatment elicited degranulation of 8% ± 1% (SD) (Figure 7), which is along spontaneous levels reported as 5% ± 1% (SD) for these experiments (spontaneous data not shown). At such low levels, it has been observed that degranulation patterns become erratic and unpredictable, which could explain why the arsenic contributions to inhibition at such high levels of piceatannol deviate from the other treatments (unpublished observations). In the absence of arsenic, the piceatannol inhibition contributed to the inhibition of degranulation in a dose dependent manner. Doses of piceatannol of 20µM, 100 µM, and 200 µM (confirmed using UV-Vis analysis; see Results section) resulted in ~13%, ~37%, and ~65%, respectively, inhibition of degranulation (Figure 7).

Co-exposure to 750 ppb arsenic and 20µM, 100 µM, and 200 µM piceatannol inhibited degranulation by ~41%, ~66%, ~77% respectively (Figure 7). This inhibition occurred in an additive fashion with 750ppb arsenic contributing a consistent inhibition of ~24% (with the exception of 200 µM) and piceatannol contributing the rest. This additive inhibition of degranulation could point to a few possible mechanisms of action. Since piceatannol acts directly at the substrate binding site of Syk to inhibit it [83, 84] it is possible that arsenic could be doing the same. Arsenate, as previously stated, has been shown to compete with free phosphate uptake and binding during phosphorylation reactions [13, 16, 18, 91, 92, 93], which lends support to a mechanism in which

piceatannol and arsenic could be collectively inhibiting Syk by competing for the tyrosine binding site of phosphate. Alternatively, it is possible that while piceatannol blocks the binding of phosphate to these tyrosine residues, arsenic could be interfering with the uptake of free-phosphate by the cell. Finally, it is also possible that arsenic could be acting indirectly to inhibit Syk by stimulating the production of ROS, which are detrimental for the activity of kinases [14].

### 4.2. Discussion of the Phospho-Syk ELISA Experiments

Optimization of the Phospho-Syk ELISA protocol has proven to be laborious, yet insightful process for our lab. We were able to eliminate our old arsenic stock as being a possible source of error, as the freshly made stock inhibited degranulation in a similar fashion as previously published data [79] and previous data reported here (Figure 4). The analysis of the human and rat SYK genes also provided valuable insight while eliminating a possible source of error in the optimization of our experiments. The high degree of homology between these genes, and the proteins they produced, made us confident that anti-human Syk antibodies would likely recognize rat Syk with a comparable degree of affinity.

The results of other optimization procedures are summarized in Figure 9 and will be further discussed here. An initial parameter tested, prior to acquisition of the CST ELISA kit, was to optimize the density of cells to be cultured the night before the experiments. The target confluence of these dishes was to be between 80-90% as recommended by the manufacturers of the ELISA kit and the densities tested were scaled up from our own experiments on 96-well microplates. Upon microscope inspection of various replicated dishes, it was concluded that cells were to be cultured at $11.375 \times 10^6$ cells per dish and

incubated overnight prior to harvesting for the ELISA experiments. The concentration of the detergent in our lysis buffers was also evaluated and optimized. Although the kit included a lysis buffer, we decided to test lower concentrations of the lysis detergent TX-100 in an effort to disturb the fragile phosphorylation events that we being targeted. It was found that the combination of scrapping and a 1% TX concentration found the manufacturers lysis buffer) of lysis buffer was crucial for proper cell lysis. The recommendations of the manufacturer were then followed in this regard as they produced the most substantial lysis of the treated cells.

Optimization of the protocol included within, however, is far from complete. Our group suspects that the sensitization, stimulation, and exposure steps (the most sensitive steps of the procedure) are likely to be the source of variability in our data. Our first issue with the optimization of these steps was the sensitization of our cultured cells. For most other experiments we are accustomed to using monoclonal anti-DNP IgE antibodies over the period of one hour immediately after the cells have cultured overnight. These antibodies are manufactured by Sigma-Aldrich and have had a tendency to cluster during long incubation times (unpublished observation). As we continue to optimize our experiments we are worried that these antibodies are not sensitizing cells properly and thus depriving the full extent of degranulation when they are stimulated. A possible solution to this issue has been proposed, and is currently in the process of being implemented. The Baird-Holowka lab (Cornell University, Ithaca, NY, USA) has kindly donated a stock of in-house produced and purified anti-DNP IgE antibodies that do not exhibit the aggregation issues of the Sigma IgE. These antibodies will enable for the sensitization to occur overnight, as it is often recommended when sensitizing RBLs, and

perhaps maximize the chances of catching a glimpse into the short lived window of phosphorylation of these vital PTKs.

A second possible source of variability in our data refers to the time and procedure involving the stimulation of the cells with DNP-BSA. Several publications argued that Syk phosphorylation was maximal upon 2 min stimulation with antigen and decreased significantly thereafter [74, 82, 83]. We carried out a pair of ELISA experiments to verify these finding with stimulation times of 2 min and 5 min but the resulting the data contradicted itself (data not shown). In the end we concluded we would continue using the 5 min stimulation as it exhibited the largest percentage increase over spontaneous in the majority of experiments carried out thereafter. This part of the protocol is of vital importance and more effort should be taken to optimize the incubation time of stimulation.

A third possible source of error in our Phospho-Syk ELISA protocol is the lysis procedure that occurs immediately after stimulation. Upon the crosslinking of the receptors and the recruitment of the PTKs there is a rapid phosphorylation of these PTKs that helps in propagation and enhancement of the stimulation signal. Almost immediately upon the activation of these PTKs, proteases and phosphatases begin dephosphorylating these PTKs to return them to their original inactivated state (see Introduction for more details). In an effort to conserve the phosphorylated state of Syk, our lysis buffer contains many anti-phosphatases and anti-proteases such as sodium orthovanadate (protein tyrosine phosphatases inhibitor), β-glycerophosphate (serine-threonine phosphatase inhibitor), leupeptin (inhibitor of serine and cysteine proteases), sodium pyrophosphate (Ser/Thr phosphatase inhibitor). Along with these vital components in the buffer, it was

also advised by the manufacturing company that all lysis steps are carried out promptly and at "ice-cold" conditions as to preserve the phosphorylated proteins. Within this crucial handling of the lysates we encounter the sonication step of cells scraped off the bottom of the treatment dishes. This sonication procedure provided many issues in terms of timing, loss of lysate volume due to splashing or excessive bubbling, and the sample heating from repetitive sonication. The latter issues were resolved by switching to more voluminous tubes and maintaining these lysate tubes submerged in a water-ice slurry during the whole sonication procedure. The issue of the timing, however, remained an elusive issue that we attempted to address. It was concluded that that sonicating the lysates at 35 Watts 3 times for 5 seconds with 10 seconds breaks in between resulted in the fastest sonication procedure that resulted in full cell lysis (Figure 9). These changes, as well as an acquired expertise with the protocol, have resulted in improved data yields that allowed us to make preliminary conclusions about the possible mechanism of arsenic toxicity in mast cell degranulation.

Preliminary data from the ELISA experiments yielded promising results. In the presence of 750 ppb arsenic, there was an observed decrease in the phosphorylation of Syk as measured by our ELISA. This experiment included two biological controls per treatment as well as a third procedural repeat for both antigen stimulated samples and the spontaneous control samples. It is difficult to make conclusions with much confidence as these results showed a high variability amongst the samples and was unable to reach statistical significance at any considerable level. However, as preliminary results they are promising and could provide some insight into the mechanism of mast cell inhibition by arsenic. If these results can be replicated, then we could potentially conclude that As is

inhibiting degranulation by interfering with the phosphorylation of Syk. Possible mechanisms for this interference could be direct as is the case with the isostructural competition of arsenate with free-phosphate as discussed in the discussion of the combined piceatannol-arsenic assays and reported across many model organisms [13,14,16, 92]. Another direct way in which As could be acting is by interacting with sulfydryl groups of proteins. A study found that arsenite interacted with sulfhydryl groups of certain proteins, causing detrimental structural modification or denaturation [92, 92, 94]. These structural modifications, as reported by Akter *et al*, can be a vital source of protein inactivation across many organisms [95]. Since both human and rat Syk contain numerous cysteine residues, five of which are located specifically in its kinase domain, inactivation via sulfhydryl interaction is a realistic possibility that should be considered (Figure 12). Our data from the piceatannol-arsenic combination assays presented above, as well as the preliminary ELISA results, appear to point towards a more direct mode of action for arsenic-induced inhibition of degranulation. Since arsenic was found to have an additive effect with piceatannol and a possible specific interference in Syk phosphorylation, it is possible that As could be inhibiting Syk by directly blocking the sites of Syk phosphorylation or by inactivating Syk altogether through structural modifications caused by sulfhydryl interactions.

There still exists the possibility that arsenic could be acting indirectly to inhibit Syk. As previously stated, arsenic could also be inhibiting the phosphorylation of Syk indirectly through the stimulation of oxyradical production [13, 16, 20, 93]. These ROS, primarily found to be superoxide, hydroxyl radicals and $H_2O_2$, have been correlated with damaging amino acids, purine nucleotides, nucleic acids, and proteins [93]. It is possible

that arsenic could be stimulating the production of these harmful radicals and thus the inactivation of not just Syk but many other molecules in the periphery. More experiments will need to be carried out before a mechanism of arsenic-induced inhibition can be elucidated.

The implications of these results can help researchers better understand the mode of arsenic toxicity that is likely to not be organism specific. If arsenic, in fact, does inhibit Syk in a direct manner, then it is possible that it may be inhibiting other similar molecules in the same manner. Furthermore, since arsenic has already been shown to inhibit such a vital pathway in allergy and asthma development, then it is possible for Syk to be used a drug target to treat these diseases. By pharmacologically mimicking the effect of arsenic on Syk, in theory, it could be possible to develop a drug to inhibit the degranulation of mast cells and perhaps alleviate the burden that hypersensitive continues to have in developed countries.

## 5. References


1. **Gomez-Caminero A**, Howe P, Hughes M, Kenyon E, Lewis DR, Moore M, Ng J, Aitio A, Becking G. 2001. Environmental Health Criteria 224 Arsenic and Arsenic Compounds. World Health Organization Geneva. Second edition.

2. **Onishi H.**1969. Arsenic. In: Wedepohl KH ed. Handbook of Geochemistry, Vol. II-2. New York, Springer.

3. **Boyle RW**, Jonasson IR. 1973. The Geochemistry Of Arsenic and its Use as an Indicator Element in Geochemical Prospecting. J Geochem Explor 2: 251–296.

4. **Barchowsky A**, Roussel RR, Klei LR, James PE, Ganju N, Smith KR, Dudek EJ. 1999. Low Levels of Arsenic Trioxide Stimulate Proliferative Signals in Primary Vascular Cells without Activating Stress Effector Pathways. Toxicol Appl Pharmacol **159:** 65-75.

5. **Styblo M**, Del Razo LM, Vega L, Germolec DR, LeCluyse EL, Hamilton GA, Reed W, Wang C, Cullen WR, Thomas DJ. 2000. Comparative Toxicity of Trivalent and Pentavelent Inorganic and Methylated Arsenicals in Rat and Human Cells. Arch Toxicol **74:** 289-299.

6. **Chou S, Harper C, Ingerman L, Llados F., Colman J, Chappell L, Osier M, Odin M, Sage G.** 2007. Toxicological Profile for Arsenic. Agency for Toxic Substances and Disease Registry: Atlanta, GA.

7. **Chen SL**, Dzeng SR, Yang MH, Chiu KH, Shieh GM, Wai CM. 1994. Arsenic Species in Groundwaters of the Blackfoot Disease Area, Taiwan. Environ Sci Technol **28(5):**877−881.

8. **Chen CC**, Grimbaldeston MA, Tsai M, Weissman IL, Galli SJ. 2005. Identification of Mast Cell Progenitors in Adult Mice. PNAS 102 (32): 11408–11413.

9. **Wong WWK**, Chung SWC, Chan BTP, Ho YY, Xiao Y. 2013. Dietary Exposure to Inorganic Arsenic of the Hong Kong Population: Results of the First Hong Kong Total Diet Study. Food Chem Toxicol 51: 379-385.

10. **Consumer Report Magazine.** 2012. Arsenic in your food; Our findings show a real need for federal standards for this toxin. Consumer Report Magazine. November 2012 issue.

11. **Ratnaike RN.** 2003. Acute and Chronic Arsenic Toxicity. Postgrad. Med. J. **79:** 391-396.

12. **Smith AH, Hopenhayn-Rich C, Bates MN, Goeden HM, Hertz-Picciotto I, Duggan HM, Wood R, Kosnett MJ, Smith MT.** 1992. Cancer Risks from Arsenic in Drinking Water. Environmental Health Perspectives. **97:** 259-267.

13. **Qian Y, Castranova V, Shi X.** 2003. New Perspectives in Arsenic-Induced Cell Signal Transduction. Journal of Inorganic Biochemistry. **96**: 271-278.

14. **Druwe IL, Vaillancourt RR.** 2010. Influence of Arsenate and Arsenite on Signal Transduction Pathways: an Update. Arch Toxicol. **84:** 585-596.

15. **Soto-Peña GA, Vega L.** 2008. Arsenic Interferes with the Signaling Transduction Pathway of T-cell Receptor Activation by Increasing Basal and Induced Phosphorylation of Lck and Fyn in Spleen Cells. Toxicology and Applied Pharmacology. **230** (2): 216-226.

16. **Ventura-Lima J, Bogo MR, Monserrat JM.** 2011. Arsenic Toxicity in Mammals and Aquatic Animals: A Comparative Biochemical Approach. Ecotoxicology and Environmental Safety. **74**: 211-218.

17. **Antoine F, Ennaciri J, Girard D.** 2010. Syk is a Novel Target of Arsenic Trioxide (ATO) and is Involved in the Toxic Effect of ATO in Human Neutrophils. Toxicology in Vitro. **24:** 936-941.

18. **DeMaster EG, Mitchell RA.** 1973. A Comparison of Arsenate and Vanadate as Inhibitors or Uncouplers of Mitochondrial and Glycolytic Energy Metabolism. Biochemistry. **12** (19): 3616-3621.

19. **Urb M, Sheppard DC.** 2012. The Role of Mast Cells in the Defense Against Pathogens. PLoS Pathog **8(4):** e1002619. doi:10.1371/journal.-ppat.1002619

20. **Liu SX, Athar M, Lippai I, Waldren C, Hei TK.** 2001. Induction of Oxyradicals by Arsenic: Implication for Mechanism of Genotoxicity. PNAS. **98 (4):** 1643-1648.

21. **Kitamura Y, Shimada M, Hatanaka K, Miyano Y.** 1977. Development of Mast Cells from Grafted Bone Marrow Cells in Irradiated Mice. Nature. **268 (5619):** 442-443.

22. **Puxeddu I, Piliponsky AM, Bachelet I, Levi-Schaffer F.** 2003. Mast Cells in Allergy and Beyond. The International Journal of Biochemistry & Cell Biology. **35:** 1601–1607

23. **Rivera J, Olivera A.** 2008. A Current Understanding of FcεRI-Dependent Mast Cell Activation. Current Allergy and Asthma Reports. **8:** 14-20.

24. **Kraft S, Kinet J.** 2007. New Developments in FcεRI Regulation, Function and Inhibition. Nature Reviews: Immunology. **7:** 365-378.

25. **Kopeć A, Panaszek B, Fal AM.** 2006. Intracellular Signaling Pathways in IgE-Dependent Mast Cell Activation. Arch. Immunol. Ther. Exp. **54:** 393-401.

26. **Wesolowski J, Paumet F.** 2011. The Impact of Bacterial Infection on Mast Cell Degranulation. Immunol. Res. **51:** 215-226.

27. **Amin K.** 2012. The Role of Mast Cells in Allergic Inflammation. Respiratory Medicine. **106**: 9-14.

28. **Bugajev V, Bambousková M, Dráberová L, Dráber P.** 2010. What Precedes the Initial Tyrosine Phosphorylation of the High Affinity IgE Receptor in Antigen-Activated Mast Cell? FEBS letters. **584:** 4949-4966.

29. **Sanderson MP, Wex E, Kono T, Uto K, Schnapp A.** 2010. Syk and Lyn Mediate Distinct Syk Phosphorylation Events in FcεRI- Signal Transduction: Implications for Regulation of IgE-Mediated Degranulation. Molecular Immunology. **48:** 171-178.

30. **Xiao W, Nishimoto H, Hong H, Kitaura J, Nunomura S, Maeda-Yamamoto M, Kawakami Y, Lowell C, Chisei R, Kawakami T.** 2005. Positive and Negative Regulation of Mast Cell Activation by Lyn via the FcεRI. The Journal of Immunology. **175:** 6885-6892.

31. **Siraganian RP, McGivney A, Barsumian EL, Crews FT, Hirata F, Axelrod J.** 1982. Variants of the Rat Basophilic Leukemia Cell Line for the Study of Histamine Release. Fed Proc. **41:** 30-34.

32. **Fewtrell C, Kessler A, Metzger H.** 1979. Comparative Aspects of Secretion from Tumor and Normal Mast Cells. Adv. Inflamm. Res. **1:** 205–221.

33. **Metzger H, Alcaraz G, Hohman R, Kinet JP, Pribluda V, Quarto R**. 1986. The Receptor with High-Affinity for Immunoglobulin-E. Annu. Rev. Immunol. **4:** 419–470.

34. **Passante E, Ehrhardt C, Sheridan H, Frankish N.** 2009. RBL-2H3 Cells are an Imprecise Model for Mast Cell Mediator Release. Inflammation Research: Official Journal of The European Histamine Research Society ... [Et Al.]. **58:**611-618.

35. **Naal RMZG, Tabb J, Holowka D, Baird B.** 2004. In Situ Measurement of Degranulation as a Biosensor Based on RBL-2H3 Mast Cells. Biosensors and Bioelectronics. **20:** 791–796

36. **Froese A, Helm RM, Conrad DH, Isersky C, Ishizaka T, Kulczycki A.** 1981. Immunology. **46:** 107-116.

37. **Swieter M, Midura RJ, Nishikata H, Oliver C, Berenstein EH, Mergenhagen SE, Hascall VC, Siraganian RP.** 1993. Mouse 3T3 Fibroblasts Induce Rat Basophilic Leukemia (RBL-2H3) Cells to Acquire Responsiveness to Compound 48/80. Journal of Immunology. **150:** 617-624.

38. **Poulsen LK, Hummelshoj L.** 2007. Triggers of IgE class Switching and Allergy Development. Annals of Medicine. **39:** 440-456.

39. **Samitas K, Lötvall J, Bossios A.** 2010. B Cells: From Early Development to Regulating Allergic Diseases. Arch. Immunol. Ther. Exp. **58:** 209-225.

40. **Gould HJ, Sutton BJ, Beavil AJ, Beavil RL, McCloskey N, Coker HA, Fear D, Smurthwaite L.** 2003. The Biology of IgE And The Basis Of Allergic Disease. **21:** 579-628.

41. **Blank U, Rivera J.** 2004 The Ins and Outs of IgE-Dependent Mast-Cell Exocytosis. TRENDS in Immunology. **25 (5):** 266-273.

42. **Kawakami T, Galli SJ.** 2002. Regulation of Mast-Cell and Basophil Function and Survival by IgE. Nature Reviews. **2:** 773-786.

43. **Kinet J.** 1999. The High-affinity IgE Receptor (FcεRI): From Physiology to Pathology. Annu. Rev. Immunol. **17:** 931-972.

44. **Turner H, Kinet J.** 1999. Signalling Through the High-Affinity IgE Receptor FcεRI. Nature. **402:** 24-30.

45. **Kuby J.** 1997. Immunology. W. H. Freeman and Company: New York.

46. **Okayama Y, Kashiwakura JI, Matsuda A, Sasaki-Sakamoto T, Nunomura S, Yokoi N, Ebihara N, Kuroda K, Ohmori K, Saito H, Ra C.** 2012. The Interaction Between Lyn and Fcεriβ is Indispensable for Fcεri-Mediated Human Mast Cell Activation. Allergy. **67:** 1241-1249.

47. **Pribluda VS, Pribluda C, Metzger H.** 1994. Transphosphorylation as the Mechanism by which the High-Affinity Receptor for IgE is Phosphorylated Upon Aggregation. Pro. Natl. Acad. Sci. **91:** 11246-11250.

48. **Young RM, Zheng X, Holowka D, Baird B**. 2004. Reconstitution of Regulated Phosphorylation of Fcepsilon RI by a Lipid Raft-Excluded Protein Tyrosine Phosphatase. *J Biol Chem*. **280 (2):** 1230-1235.

49. **Nishizumi H, Yamamoto T.** 1997. Impaired Tyrosine Phosphorylation and Ca2+ Mobilization, but Not Degranulation, in Lyn-Deficient Bone Marrow-Derived Mast Cells. Journal of Immunology. **97:** 2350-2355.

50. **Zhang W, Trible RP, Zhu M, Liu SK, McGlade J, Samelson LE.** 2000. Association of Grb2, Gads, and Phospholipase C-g1 with Phosphorylated LAT Tyrosine Residues. Journal of Biological Chemistry. **275 (30):** 23355-23361.

51. **Kozak JA, Kerschbaum HH, Cahalan MD.** 2002. Distinct Properties of CRAC and MIC Channels in RBL Cells. J Gen Physiol. **120 (2):** 221-235.

52. **Hoth M, Penner R.** 1992. Depletion of intracellular calciumstores activates a calcium current in mast cells. *Nature.* **355:**353–356.

53. **Roos J, DiGregorio PJ, Yeromin AV, Ohlsen K, Lioudyno M, Zhang S, Safrina O, Kozak JA, Wagner SL, Cahalan MD, Veliçelebi G, Stauderman KA**. 2005.

STIM1, an Essential and Conserved Component of Store-Operated $Ca^{2+}$ Channel Function. J Cell Biol. **169 (3):** 435-445.

54. **Baba Y, Nishida K, Fujii Y, Hirano T, Hikida M, Kurosaki T.** 2008. Essential Function for the Calcium Sensor STIM1 in Mast Cell Activation and Anaphylactic Responses. Nat Immunol. **9 (1):** 81-88.

55. **Liou J, Kim ML, Heo WD, Jones JT, Myers JW, Ferrell JE Jr, Meyer T**. 2005. STIM is a Ca2+ Sensor Essential for Ca2+-Store-Depletion-Triggered Ca2+ Influx. Curr Biol. **15 (13):** 1235-1241.

56. **Ludowyke RI, Peleg I, Beaven MA, Adelstein RS.** 1989. Antigen-Induced Secretion of Histamine and the Phosphorylation of Myosin by Protein Kinase C in Rat Basophilic Leukemia Cells. J Biol Chem. **264(21):** 12492-12501.
57. **Holst J, Sim AT, Ludowyke RI.** 2002. Protein Phosphatases 1 and 2A Transiently Associate with Myosin During the Peak Rate of Secretion from Mast Cells. Mol Biol Cell. **13(3):** 1083-1098.
58. **Buxton DB, Adelstein RS.** 2000. Calcium-Dependent Threonine Phosphorylation of Nonmuscle Myosin in Stimulated RBL-2H3 Mast Cells. J Biol Chem. **275(44):** 34772-34779.

59. **Jena BP.** 2011. Role of SNAREs in Membrane Fusion. Adv Exp Med Biol. **713:** 13-32.

60. **Tadokoro S, Nakanishi M, Hirashima N.** 2010. Complexin II Regulates Degranulation in RBL-2H3 Cells by Interacting with SNARE Complex Containing Syntaxin-3. Cell Immunol. **261(1):** 51-56.

61. **Woska JR Jr, Gillespie ME.** 2011. Small-Interfering RNA-Mediated Identification and Regulation of the Ternary SNARE Complex Mediating RBL-2H3 Mast Cell Degranulation. Scand J Immunol. **73(1):** 8-17.

62. **Epp N, Rethmeier R, Kramer L, Ungermann C.** 2011. Membrane Dynamics and Fusion at Late Endosomes and Vacuoles- Rab Regulation, Multisubunit Tethering Complexes and SNAREs. Eur J Cell Biol. **90 (9):** 779-785.

63. **Choi WS, Kim YM, Combs C, Frohman MA, Beaven MA.** 2002. Phospholipases D1 and D2 Regulate Different Phases of Exocytosis in Mast Cells. J. Immunol. **168:** 5682-5689.

64. **Ingley E.** 2012. Functions of the Lyn Tyrosine Kinase in Health and Disease. Cell Communication and Signalling. **10:** 21-32.

65. **Xu W, Doshi A, Lei M, Eck MJ, Harrison SC.** 1999. Crystal Structures of c-Src Reveal Features of its Autoinhibitory Mechanism. Molecular Cell. **3:** 629-638.

66. **Futami M, Zhu QS, Whichard ZL, Xia L, Ke Y, Neel BG, Feng GS, Corey SJ** 2011. G-CSF Receptor Activation of the Scr Kinase Lyn is Mediated by Gab2 Recruitment of the Shp2 Phosphatase. Blood. **118:** 1077-1086.

67. **Gilfillan AM, Rivera J.** 2009. The Tyrosine Kinase Network Regulating Mast Cell Activation. Immunological Reviews. **228:** 149-169.

68. **Hernandez-Hansen V, Smith AJ, Surviladze Z, Chigaev A, Mazel T, Kalesnikoff J, Lowell CA, Krystal G, Sklar LA, Wilson BS, Oliver JM.** 2004. Dysergulated, FcεRI Signaling and Altered Fyn and SHIP Activities in Lyn-Deficient Mast Cells. Journal of Immunology. **173:** 100-112.

69. **Kovarova M, Wassif CA, Odom S, Liao K, Porter FD, Rivera J.** 2006. Cholesterol Deficiency in a Mouse Model of Smith-Lemli-Opitz Syndrome Reveals Increased Mast Cell Responsiveness. JEM. **203 (5):** 1161-1171.

70. **Turner M, Schweighoffer E, Colucci F, Di Santo JP, Tybluwicz VL.** 2000. Tyrosine Kinase SYK: Essential Functions for Immunoreceptor Signaling. Immunology Today. **21 (3):** 148-154.

71. **Chu DH, Morita CT, Weiss A.** 1998. The Syk Family of Protein Tyrosine Kinases In T-Cell Activation and Development. Immunological Reviews. **165:** 167-180.

72. **Zoller KE, MacNeil IA, Brugge JS.** 1997. Protein Tyrosine Kinase Syk and ZAP-70 Display Distinct Requirements for Src Family Kinase in Immune Response Receptor Signal Transduction. J Immunol. **158(4):** 1650-1659.

73. **Furlong MT, Mahrenholz AM, Kim KH, Ashendel CL, Harrison ML, Geahlen RL.** 1997. Identification of the Major Sites of Autophosphorylation of the Murine Protein-Tyrosine Kinase Syk. Biochim Biophys Acta. **1355(2):** 177-190.

74. **Chan AC, Dalton M, Johnson R, Kong GH, Wang T, Thoma R, Kurosaki T.** 1995. Activation of ZAP-70 Kinase Activity by Phosphorylation of Tyrosine 493 is Required for Lymphocyte Antigen Receptor Function. EMBO J. **14(11):** 2499-2508.

75. **Zhang J, Berenstein EH, Evans RL, Siraganian RP.** 1996. Transfection of Syk Protein Tyrosine Kinase Reconstitutes Hight Affinity IgE Receptor-mediated Degranulation in a Syk-negative Variant of Rat Basophilic Leukemia RBL-2H3 Cells. J. Exp. Med. **184:** 71-79.

76. **Grodzki ACG, Moon KD, Berenstein EH, Siraganian RP.** 2009. FCεRI- Induced Activation by Low Antigen Concentrations Results in Nuclear Signals in the Absence of Degranulation. Molecular Immunology. **46:** 2539-2547.

77. **De Castro RO.** 2011. Regulation and Function of Syk Tyrosine Kinase in Mast Cell Signaling and Beyond. Journal of Signal Transduction. **2011:** doi:10.1155/2011/507291.

78. **Zhang J, Kimura T, Siraganian RP.** 1998. Mutations in the Activation Loop Tyrosines of Protein Tyrosine Kinase Syk Abrogate Intracellular Signaling But Not Kinase Activity. J. Immunol. **161:** 4366-4374.

79. **Hutchinson LM, Trinh BM, Palmer RK, Preziosi CA, Pelletier JH, Nelson HM, Gosse JA.** 2011. Inorganic Arsenite Inhibits IgE Receptor-Mediated Degranulation of Mast Cells. Journal of Applied Toxicology. **31**: 231-241.

80. **Hutchinson LM.** 2011. Inorganic Arsenite Inhibits Allergic Signal Transduction in Mast Cells. Graduate Thesis. The Graduate School, University of Maine.

81. **Pelletier JH.** 2011. Comparative analysis of toxicant effects on several distinct transduction pathways that all lead to degranulation in rat-derived mast cells as a model system. Honors Undergraduate Thesis. The Honors College, University of Maine.

82. **Geahlen RL, McLaughlin JL.** 1989. Piceatannol (3,4,3', 5'- tetrahydroxy-trans-stilbene) is a Naturally Occurring Protein-Tyrosine Kinase Inhibitor. Biochemical and Biophysical Research Communications. **165:** 241-245.

83. **Oliver JM, Burg DL, Wilson BS, McLaughlin JL, Geahlen RL.** 1994. Inhibition of Mast Cell FcεR1-Mediated Signaling and Effector Function by the Syk-Selective Inhibitor, Piceatannol. The Journal of Biological Chemistry. **269 (47):** 29697-29703.

84. **Matsuda H, Tewtrakul S, Morikawa T, Yoshikawa M.** 2004. Anti-Allergic Activity of Stilbenes From Korean Rhubarb (*Rheum Undulatum* L.): Structure Requirements for Inhibition of Antigen-Induced Degranulation and their Effects on the Release of TNF-A and IL-4 in RBL-2H3 Cells. Bioorganic & Medicinal Chemistry. **12:** 4871-4876.

85. **Suzuki Y, Yoshimaru T, Yamashita K, Matsui T, Yamaki M, Shimizu K.** 2001. Exposure of RBL-2H3 Mast Cells to $Ag^{+}$ Induces Cell Degranulation and Mediator Release. Biochemical and Biophysical Research Communications. **283:** 707-714.

86. **Pfeiffer JR, Oliver JM.** 1994. Tyrosine Kinase-Dependent Assembly of Actin Plaques Linking FcεR1 Cross-Linking to Increased Cell Substrate Adhesion in RBL-2H3 Tumor Mast Cells. J Immunol. **152**:270-279.

87. **Li Z, Yang X, Dong S, Li X.** 2012. DNA Breakage Induced by Piceatannol and Copper(II): Mechanism and Anticancer Properties. Oncology Letters. **3:** 1087-1094.

88. **Hardy RR.** 1986. Purification and characterization of monoclonal antibodies. Handbook of Experimental Immunology. D. M. Weir. Oxford, Blackwell Scientific Publications: 13.1-13.13.

89. **Nelson DL, Cox MM.** 2008. Lehninger Principles of Biochemistry 5th Edition. W. H. Freeman and Company: New York.

**90. Hornbeck P, Winston SE, Fuller SA.** 2001. Enzyme-Linked Immunosorbent Assays UNIT 11.2 (ELISA). Curr Protoc Mol Biol. **Chapter 11:Unit11.2. doi: 10.1002/0471142727.mb1102s15.**

91. **Egdal RK, Raber G, Bond AD, Hussain M, Espino MPB, Francesconi KA, McKenzie CJ.** 2009. Selective Recognition and Binding of Arsenate over Phosphate. Dalton Trans. **44:** 9718–9721.

92. **Hutchcroft JE, Geahlen RL, Deanin GG, Oliver JM.** 1992. FcεR1-Mediated Tyrosine Phosphorylation and Activation of the 72-kDa Protein-Tyrosine, PTK72, in RBL-2H3 Rat Tumor Mast Cells. Proc Natl Acad Sci USA. **89 (19):** 9107-9111.

93. **Finnegan PM, Chen W.** 2012. Arsenic Toxicity: the Effects on Plant Metabolism. Front Physiol. **3 (182)** doi: 10.3389/fphys.2012.00182. Epub 2012 Jun 6.

94. **Wang YC, Chaung RH, Tung LC.** 2004. Comparison of the Cytoxicity Induced by Different Exposure to Sodium Arsenite in Two Fish Cell Lines. Aquat Toxicol. **63(1):** 67-79.

95. **Akter KF, Owens G, Davey DE, Naidu R.** 2005. Arsenic Speciation and Toxicity in Biological Systems. Rev Environ Contam Toxicol. **184:** 97-149.

**Author's Biography**

Alejandro Velez Lopez Naranjo Ospina, was born in Pereira, Colombia on May 7th, 1990. He was raised in several cities in Colombia and move to Johnstown, New York at the age of twelve. He graduated high school from New Berlin West high school in 2008 and decided to follow his family to Hampden, Maine for college. While at the University of Maine, he founded *Iota Nu Kappa Multicultural Fraternity* and worked closely with the Office of Multicultural Programs to serve the campus and the surrounding community. As a biochemistry major, he has received the *INBRE Functional Genomics Fellowship* and the *Professor Frederick H. Radke Award* and was invited to participate in the *Summer Training in Academic Research and Scholarship* program through a partnership between Brigham and Women's Hospital and Harvard Medical School.

Upon graduation, Alejandro will be attending graduate school to acquire a master in public health with hopes of attending medical school thereafter.